INSTITUTO SUPERIOR
DE CIÊNCIAS DA SAÚDE
NORTE

CESPU

INSTITUTO SUPERIOR DE CIÊNCIAS DA SAÚDE-NORTE

DEPARTAMENTO DE CIÊNCIAS

Mestrado em Terapias Moleculares

INSIGHTS INTO THE FUNCTION OF TRANSTHYRETIN IN THE PERIPHERAL NERVE AND BONE BIOLOGY

Filipa Sofia Franquinho Ferreira

Gandra, 2010

Filipa Sofia Franquinho Ferreira

INSIGHTS INTO THE FUNCTION OF TRANSTHYRETIN IN THE PERIPHERAL NERVE AND BONE BIOLOGY

Dissertação para a obtenção do grau de Mestre em Terapias Moleculares pelo Instituto Superior de Ciências da Saúde-Norte

Trabalho de tese realizado sob a orientação de Mónica Luísa Ribeiro Mendes de Sousa.

Instituto Superior de Ciências da Saúde-Norte
Departamento de Ciências
2010

ACKNOWLEDGMENTS

Agradeço à Mónica, minha orientadora, por ter acreditado no meu trabalho, por tudo o que me ensinou e pelo carinho com que me acolheu desde o primeiro dia em que entrei para o seu grupo.

À Carolina e à Filipa Nunes por terem partilhado o seu trabalho comigo.

À Márcia por me ter contagiado com o seu entusiasmo, à Carla e Pedro Brites pela partilha de experiências. Ao Fernando e à Catarina pela amizade. Ao Sérgio, pela ajuda e disponibilidade.

À Marta, Nélson, Nádia, Marisa e Carlos pela sempre boa disposição e simpatia.

Às minhas colegas e, principalmente, grandes amigas Dolores e Vera por me terem encorajado a iniciar esta caminhada.

Agradeço aos meus pais e avós por todo o apoio que me deram. À Cláudia, pela paciência.

Ao Pedro, por estar sempre ao meu lado.

Agradeço aos coordenadores do Mestrado em Terapias Moleculares por me terem acolhido como aluna.

Agradeço ao Instituto de Biologia Molecular e Celular por me ter proporcionado as condições para o desenvolvimento desta tese.

TABLE OF CONTENTS

ABSTRACT

Transthyretin (TTR) is synthesized by the liver and choroid plexus of the brain that contribute to the plasma and cerebrospinal fluid pool of the protein. When mutated, TTR is associated to familial amyloid polyneuropathy (FAP), a neurodegenerative disease characterized by TTR deposition in the form of aggregates and extracellular deposits, particularly in the peripheral nervous system (PNS). TTR deposition in the PNS leads to fatal neuronal loss. In this study, we aimed to search the biological functions for TTR in the nerve (that could explain its preferential deposition in the PNS, when mutated) and the biological consequences of the lack of TTR in TTR KO mice. Under physiological conditions, we found no morphometric differences in the sciatic nerve of WT and TTR KO littermates that could explain the sensorimotor impairment of TTR KOs. However, after injury, we show that TTR KO mice present a slower recovery as detected by a decreased number of myelinated and unmyelinated fibers. This slower regeneration was reversed after delivery and local expression of TTR in the nerve. Associated to the lack of TTR, TTR KO mice present a higher expression of the rate limiting enzyme in neuropeptide amidation, peptidylglycine α-amidating monooxygenase (PAM) and, consequently, higher levels of the major amidated neuropeptide – neuropeptide Y (NPY). As NPY has been related to bone remodeling and neuroproliferation, we investigated the bone and neuroproliferative phenotype of TTR KO mice. This strain showed an augmented bone mass related to a higher NPY and PAM expression during osteoblastic differentiation and in various bone cells. Regarding neuroproliferation and, despite it has been shown to be induced by NPY, no differences were found between TTR KO and WT mice.

In conclusion, we determined that TTR enhances nerve regeneration and that lack of TTR is associated with increased bone mass as a consequence of increased NPY levels and PAM expression.

RESUMO

A Transtirretina (TTR) é sintetizada pelo fígado e plexo coróide do cérebro que constituem as fontes de proteína no plasma e líquido cefalorraquidiano. Quando mutada, a TTR está associada à polineuropatia amiloidótica familiar (FAP), uma doença neurodegenerativa caracterizada pela deposição de TTR sob a forma de agregados e depósitos extracelulares, particularmente no sistema nervoso periférico (SNP). A deposição de TTR no SNP conduz a perda neuronal. Neste estudo, tivemos como objectivo identificar funções biológicas para a TTR no nervo periférico (o que pode explicar a sua deposição preferencial no SNP, quando mutada) e as consequências biológicas da ausência de TTR nos ratinhos TTR KO. Em condições fisiológicas, não verificámos diferenças morfométricas entre os nervos ciáticos dos ratinhos WT e TTR KO que pudesse explicar o défice sensório-motor dos ratinhos TTR KO. No entanto, demonstrámos que, após lesão, os ratinhos TTR KO recuperam mais lentamente como foi detectado por uma diminuição do número de fibras mielinizadas e não-mielinizadas. Esta regeneração lenta foi revertida após a administração e expressão local de TTR no nervo. Associado à ausência de TTR, os ratinhos TTR KO apresentam uma maior expressão de *peptidylglycine α-amidating monooxygenase* (PAM), a enzima que desempenha o passo limitante da amidação de neuropéptidos e, consequentemente, maiores níveis do maior neuropéptido amidado – neuropéptido Y (NPY). Como o NPY tem vindo a ser relacionado com a remodelação óssea e com a neuroproliferação, procurámos estudar o fenótipo ósseo e neuroproliferativo dos ratinhos TTR KO. Nesta estirpe verificou-se um aumento da massa óssea relacionado com o aumento da expressão de NPY e PAM durante a diferenciação osteoblástica e nos vários tipos de células ósseas. Relativamente à neuroproliferação, e apesar de ter sido demonstrado que é induzida pelo NPY, não se verificaram diferenças entre os ratinhos TTR KO e WT.

Em conclusão, verificou-se que a TTR promove a regeneração do nervo e que a ausência de TTR está associada com o aumento da massa óssea como consequência do aumento dos níveis de NPY e da expressão de PAM.

PART ONE

General Introduction

TRANSTHYRETIN

Transthyretin (TTR), which was first discovered in 1942 (Kabat et al., 1942) is a tetrameric protein composed by four identical subunits (Blake et al., 1971) with 54,980 Daltons (total molecular weight) and of 127 aminoacids (Kanda et al., 1974).

TTR is synthesized mainly by the liver and choroid plexus epithelial cells being secreted into the blood (Gitlin and Gitlin, 1975) and into the cerebrospinal fluid (CSF) (Aleshire et al., 1983), respectively. Additionally, other studies have demonstrated minor TTR synthesis by other organs such as the pancreas (Kato et al., 1985), stomach, heart, muscle, spleen (Soprano et al., 1985) and meninges (Blay et al., 1993).

TTR has a dual physiological role as a transporter (*trans*) of thyroid hormones (*thy*) and retinol-binding protein (*retin*) in the blood (figure 1).

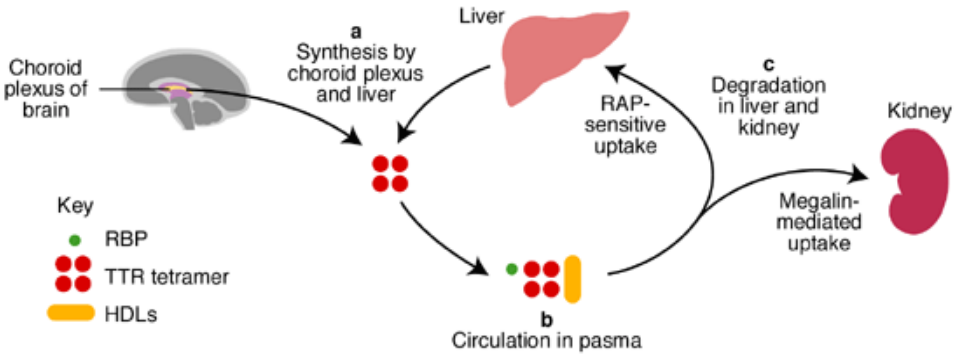

Figure 1 – Synthesis, circulation and uptake of transthyretin. (**a**) Transthyretin (TTR) (red circles) is synthesized by the choroid plexus of the brain and by the liver. The mechanisms underlying delivery and uptake of TTR within and out of the brain are not known. (**b**) The tetramer circulates in plasma bound to retinol-binding protein (RBP; green circle) thereby providing a transport function for retinol; a small proportion of TTR binds high-density lipoproteins (HDLs; yellow bar). (**c**) TTR is degraded in the kidney and liver. In the kidney tubules, TTR is taken up by megalin; in the liver, an yet unidentified receptor that binds receptor-associated protein (RAP) is responsible for TTR uptake (adapted from *Expert Reviews in Molecular Medicine © 2002 Cambridge University Press*).

Thyroid hormones, such as thyroxine (T_4) are important regulators of metabolism and normal growth. Only 15% of circulating T_4 in the human bloodstream is transported by TTR since this hormone has a higher affinity for thyroxine-binding globulin (Loun and Hage, 1992). In contrast, TTR is the major T_4 carrier both in the human and rodent CSF (about 80%).

The two structurally identical binding sites for T_4 are located between two of the four subunits in the TTR tetramer (Blake et al., 1978; Blake et al., 1974), (figure 2A).

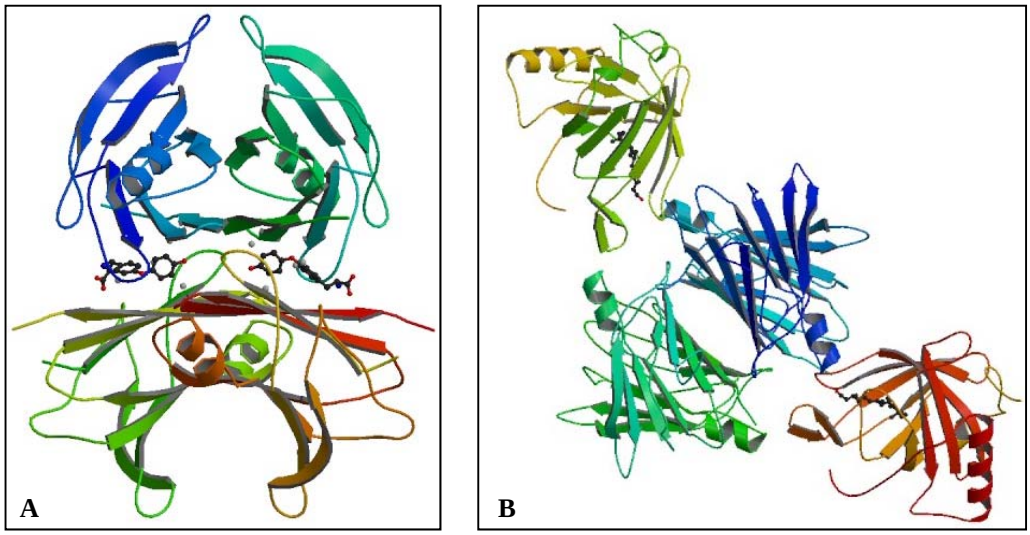

Figure 2 – Transthyretin as a hormone and vitamin transporter. (**A**) Monoclinic form of human transthyretin complexed with T_4 at the center in black (Protein Data Bank 1ICT); (**B**) TTR-RBP-retinol complex (TTR is shown in the center in blue and green, RBP in red and yellow/green in the upper left and lower right side, and retinol in black) (Protein Data Bank 1ICT).

Retinol (synthesized and secreted by the liver) is transported specifically bound to retinol binding protein (RBP) and TTR (Kanai et al., 1968). The complex TTR-RBP-retinol prevents glomerular filtration of both RBP (21,000 Da) and retinol. Though TTR tetramer has four RBP binding sites (van Jaarsveld et al., 1973), only one molecule binds to TTR under physiological conditions (figure 2B) due to physiological limitations, namely the fact that TTR is 2-3 fold more concentrated than circulating RBP in the plasma (van Bennekum et al., 2001). Retinoic acid also binds to TTR (Smith et al., 1994) but with a lower affinity.

Familial amyloid polyneuropathy (FAP)

Familial amyloid polyneuropathy (FAP) is the main neurodegenerative disease associated to mutated TTR and it was first described in 1952 by Corino de Andrade (Andrade, 1952). From the over 100 amyloidogenic TTR variants described, the most common causing FAP is Val30Met (Saraiva et al., 1984). TTR Val30Met causes systemic extracellular deposits of mutated TTR and amyloid fibrils particularly in the

peripheral nervous system (PNS) (Coimbra and Andrade, 1971a; Coimbra and Andrade, 1971b), with the exception of the brain and liver parenchyma. The extracellular amyloid deposits can be found diffusely in the PNS, involving nerve trunks, plexuses, sensory and autonomic ganglia (Hanyu et al., 1989; Said et al., 1984; Sobue et al., 1990). Following TTR deposition, axonal degeneration occurs, starting in the unmyelinated fibers and myelinated fibers of low diameter, and ultimately leading to neuronal loss at ganglionic sites (Sousa and Saraiva, 2003). FAP sensory impairment-related symptoms occur before middle age and patients die 10 to 20 years after the onset. Although liver transplantation is currently used to abolish mutant TTR production and prevent disease progression, some of the neurological lesions persist irreversible (Furtado et al., 1999)

The mechanism through wich TTR aggregates and forms amyloid fibrils is still obscure though, several studies point towards conformational changes that disrupt the tetramer into non-native monomers as the beginning of amyloid fibril formation (Bonifacio et al., 1996; Quintas et al., 1999) (figure 3).

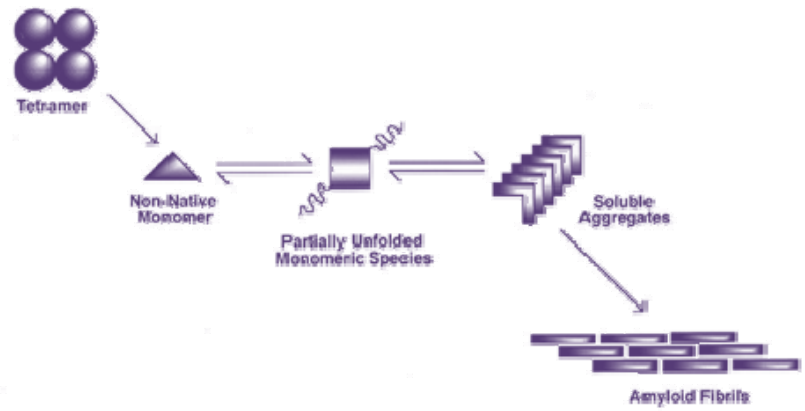

Figure 3 – Mechanism for amyloid fibril formation by TTR in physiological conditions (Quintas et al., 2001).

The fact that mutated TTR deposits preferentially in the nerve, suggests a function of this protein in this structure.

TTR knockout mice

In 1993, TTR knockout (TTR KO) mice were generated (Episkopou et al., 1993) to investigate the physiological role of TTR during embryonic development and in adult animals, specially the role of its ligands, thyroxine (T_4) and retinol. In general terms, this strain revealed to be fertile, having a normal life span and displaying no obvious phenotypic abnormalities postnatally (Episkopou et al., 1993). As expected, plasma from TTR KO mice had decreased levels of both T_4 and T_3 (Episkopou et al., 1993). In terms of thyroid hormones tissue content, no significant differences in T_4 levels were found in TTR KO mice when compared to WT mice (Palha et al., 1997). Probably underlying their euthyroid status, free T_4 was 50% increased in the serum of TTR KO mice (Palha, 2002). As such, the absence of TTR does not seem to affect thyroid hormone function. In the case of retinol, TTR KO mice were expected to have a vitamin A deficiency. Though their retinol plasma levels were below the detection level, mice lacking TTR did not show any symptoms of vitamin A deficiency (Episkopou et al., 1993). In agreement with the lack of symptoms of vitamin A deficiency, the total retinol levels in tissues were not significantly different from WT mice (Wei et al., 1995). Similarly to thyroid hormones, in the case of vitamin A, the above findings suggest that TTR KO mice present no major defects related to retinol deficiency.

TTR and the biology of the nervous system

Since the initial characterization, TTR KO mice revealed to be one of the most valuable tools to link the biology of TTR with that of the Central Nervous System (CNS) and PNS. The idea that this protein might be linked to the nervous system derived from the fact that, when mutated, it originates a neuropathy and also because, under physiological conditions, it is highly abundant in the CSF.

The first observation linking TTR to the physiology of the nervous system was the fact that TTR KO mice present a decreased anxiety-like behavior and an increased motor activity when compared to WT animals (Sousa et al., 2004a). Later, using the SHIRPA analysis (Rogers et al., 1997), it was shown that this phenotype was reversed with age. Thus, at 12 months of age, TTR KO mice had a decreased motor activity probably due to an age-dependent increase in motor discoordination (Fleming et al., 2007), (figure 4). At the sensory level, TTR KO mice had an increased latency in

response to a nociceptive noxious thermal stimulus as determined using the hot plate test (Fleming et al., 2007), further reinforcing their sensorimotor impairment.

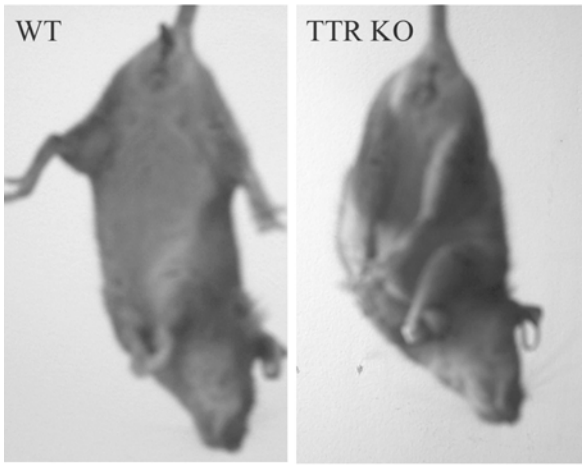

Figure 4 – TTR KO mice present motor discoordination (limb clasping) (Fleming et al., 2007).

At the molecular level, increased limbic levels of norepinephrine were shown in TTR KOs (Sousa et al., 2004a) suggesting that TTR involvement in behavior occurred through modulation of the noradrenergic system. In fact, the pathophysiology of depression has been traditionally focused on the serotoninergic and noradrenergic systems. However, growing evidence indicates that neuropeptides, in particular neuropeptide Y (NPY), may also play a role in affective diseases, such as in depression, as it has been shown that central NPY administration displays antidepressant-like activity (Heilig, 2004). In this respect, Nunes et al. reported that TTR KO have increased NPY, an anxyolytic neuropeptide.

The above data strongly suggest that TTR plays a role in the biology of the nervous system, probably not only in physiological conditions but also during the course of disease/injury.

In agreement with a function for TTR in the CNS, recent studies have implicated TTR in behavior and CNS disorders. Altered TTR levels in the CSF have been linked to neuronal dysfunctions, such as Alzheimer's disease, in which TTR in the CSF is negatively correlated with the degree of dementia (Serot et al., 1997). Although TTR has been linked to CNS pathology, the link to nerve regeneration remained to be explored.

TTR KO mice as a model for increased NPY levels

Evidence for a role of TTR in the physiology of the nervous system, namely in behavior, came from the observation that TTR knockout (KO) mice are less depressed than control mice (Sousa et al., 2004a) together with the fact that they display increased limbic levels of norepinephrine (Nunes et al., 2006).

PNS microarray analysis and immunohistochemistry revealed an up-regulation (24-fold) of peptidylglycine α-amidating monooxygenase (PAM) in dorsal root ganglion (DRG) of TTR KO compared to WT (Nunes et al., 2006). NPY is the major neuropeptide present in the mammalian brain (Pedrazzini et al., 2003) and requires C-terminal α-amidation by PAM for its activation (figure 5). Although NPY expression is not altered, TTR KO mice showed higher levels of this neuropeptide both in CNS and PNS.

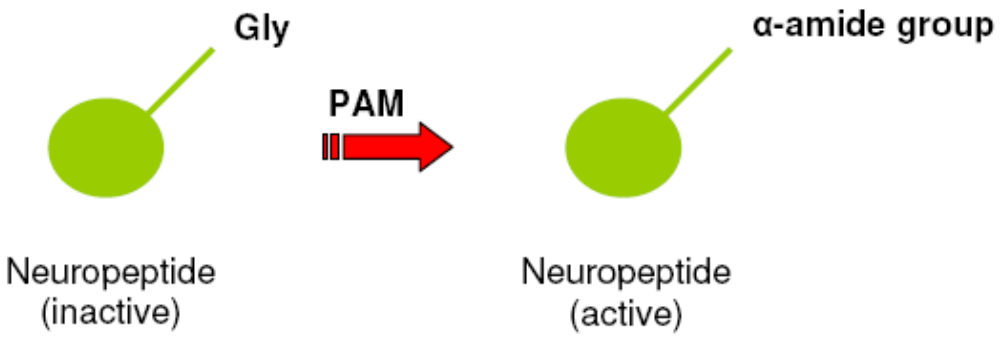

Figure 5 – Schematic representation of PAM involvement in regulating neuropeptide amidation. PAM sequentially catalyzes the conversion of glycine-extended peptides into C-terminal amidated peptides (from Nunes AF, PhD Thesis, 2007)

These findings suggest that lack of TTR interferes in the nervous system homeostasis and suggest that TTR may play a role in events related to neurodegeneration/neuroprotection in PNS diseases.

Peripheral nerve regeneration

Central Nervous System regeneration is conditioned by the glial scar (formed by astrocytes) and an inhibitory environment that blocks axonal growth after injury. In

contrast, the Peripheral Nervous System has a higher regenerative capacity which might be related to the rapid clearance of myelin debris by PNS macrophages and Schwann cells (George and Griffin, 1994; Schafer et al., 1996) providing a favorable environment for axonal growth (figure 6).

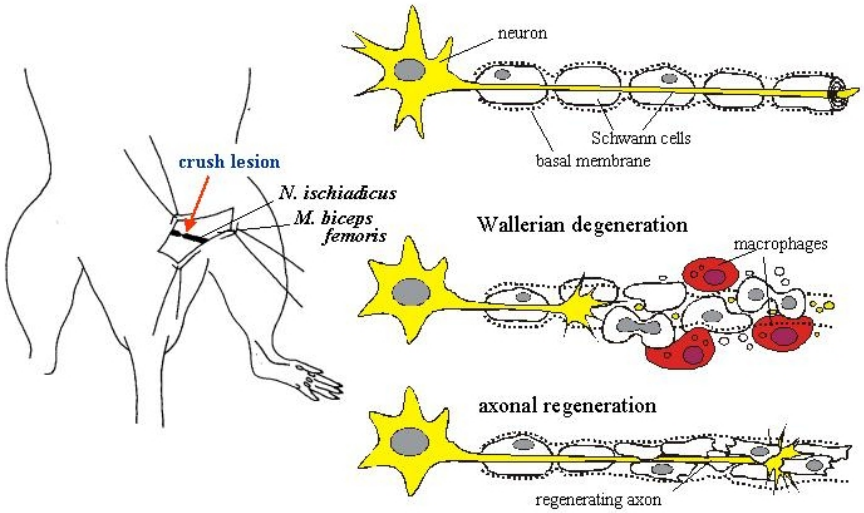

Figure 6 – Peripheral nerve regeneration. After injury, axonal integrity is disrupted and degeneration occurs. To promote axonal growth, previously myelinating Schwann cells de-differentiate, start to proliferate and producing growth factors (available at www.bio2.rwth-aachen.de/research/RERENER.htm).

It is accepted that the ability of peripheral axons to regenerate following injury relies on alterations of gene transcription and protein synthesis, although, the identity of the molecules and the mechanisms by which signals inform the cell body that the axon has been injured are still obscure.

Wallerian degeneration is a degenerative process that occurs in the distal stump of injured nerves. In the course of Wallerian degeneration, Schwann cells dedifferentiate, downregulate myelin protein synthesis in response to axonal loss (LeBlanc and Poduslo, 1990) and begin to catabolize myelin and later engulf axon fragments (figure 7).

After injury, neuronal survival is also promoted by the recruitment of macrophages that infiltrate the lesion site to phagocyte myelin debris and neurotrophins that are retrogadely transported after production at the target tissue.

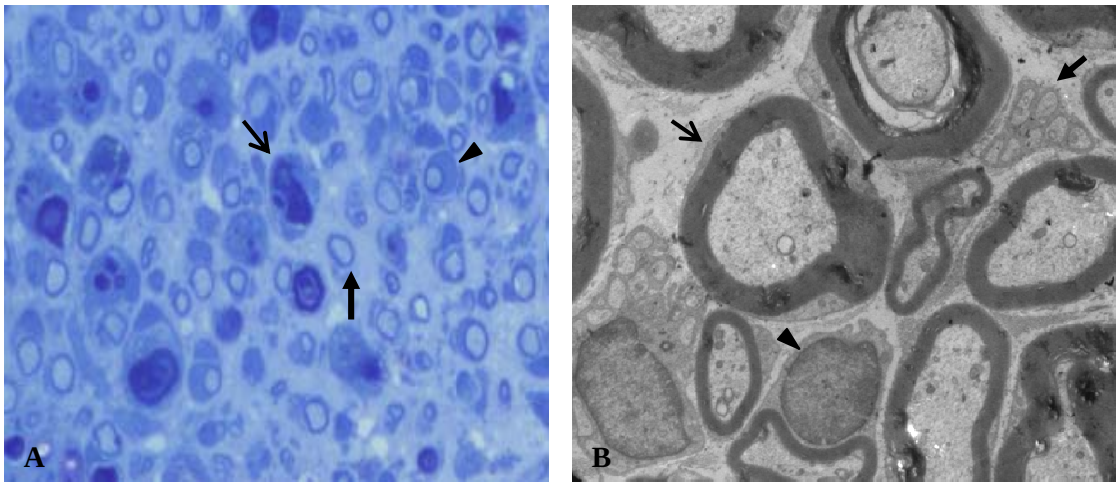

Figure 7 – Mouse sciatic nerve. (**A**) Regenerating mouse sciatic nerve stained with toluidine blue. Myelinated fibers (arrow), macrophages (open arrow) and a Schwann cell (arrowhead) at a 40x magnification. (**B**) Electron microscopy evidences the presence of unmyelinated fibers (arrow) together with myelinated fibers (open arrow) and a Schwann cell (arrowhead) surrounding a myelinated fiber (x 7000).

The injured nerve is able to regrow from the proximal stump to the distal end. This growth is supported by the transport of molecules that travel along the cell body to the tip of the axon (anterograde transport), followed by the transport of injury signals from the lesion site to the cell body (retrograde transport). The signals that reach the cell body modulate axonal elongation since injured neurons need to express proteins (such as tubulin) so that axonal growth takes place.

Following degeneration and axonal regeneration, remyelination needs to proceed and occurs in a similar process to the normal process of myelination during development.

PART TWO

Research Project

OBJECTIVES

The aim of the present work was to search the function of TTR in the peripheral nerve and bone biology.

To achieve this objective we proposed to:

- Chapter I – Assess the role of TTR in peripheral nerve biology in physiological conditions and after injury.

- Chapter II – Assess the biological consequences of increased NPY levels in TTR KO mice, specifically in bone and brain.

CHAPTER I

Assessment of TTR function in the peripheral nerve biology

INTRODUCTION

TTR function in nerve biology is not fully understood. The blood-nerve barrier (BNB) is effective in slowing the entry of proteins in the endoneurium although it does not prevent them to enter. TTR may also have access to peripheral nerves through the CSF, where it is present in high levels. In fact, Fleming et al (2009) not only reported that intravenously injected TTR is detectable in the endoneurium of both WT and TTR KO nerves, 1 to 3 days after crush, but also under physiological conditions.

According to Fleming et al (2007), under physiological conditions, TTR KO mice display limb clasping and a higher latency to respond to thermal stimulus. However, this sensorimotor impairment was not related to differences on the dendritic tree structure nor on the number of cerebellum Purkinje cells (the centre of motor coordination) (Fleming et al., 2007). Also, under physiological conditions, no significant differences were found on the total number of myelinated fibers nor in the g ratio (a measure of myelin thickness) in the sciatic nerve of young adult WT and TTR KO mice (Fleming et al., 2007), that could underlie the sensorimotor impairment of the latest. Moreover, after sciatic nerve crush, TTR KO revealed a lower motor nerve conduction velocity and locomotor activity when compared to WT (Fleming et al., 2007). These findings point towards the hypothesis that TTR KO mice have a delayed regeneration. Supporting this hypothesis, dorsal root ganglia (DRG) neurons supplemented with WT mouse serum *in vitro*, presented an increase in neurite number when compared to DRG neurons supplemented with TTR KO mouse serum. This suggests that, at least *in vitro*, TTR delivery can induce neurite outgrowth. In this respect, the internalization of TTR by sensory neurons was shown to be a clathrin-dependent endocytic process (Fleming et al., 2009), necessary for TTR to exert its neuritogenic effect.

Despite that these studies unravel a role of TTR in nerve regeneration and sensorimotor performance, morphometric analysis of regenerating WT and TTR KO nerves was lacking. Also, the effect of TTR delivery *in vivo* needed to be explored. Additionally, the mechanism through which TTR exerts its function is still unknown.

The present work aims to address the physiological effect of TTR on peripheral nerve and the biological consequences for nerve biology when TTR is lacking.

MATERIALS AND METHODS

Animals

Mice were handled according to the European Communities Council Directive (86/609/EEC) as well as to the National rules and all studies performed were approved by the Portuguese General Veterinarian Board. WT and TTR KO littermate mice as well as megalin heterozygous [MEG (+/-), were kindly provided by Dr. Thomas Willnow, Max-Delbrueck Center for Molecular Medicine, Berlin, Germany], TTR KO/MEG (+/-) littermate mice (in the 129/Sv background), and Thy 1.2-TTR transgenic mice in a TTR KO background (Sousa et al., 2004c) were obtained from the offspring of heterozygous breeding pairs and maintained at 24 ± 1^{o}C under a 12 h light/dark cycle and fed regular chow and tap water *ad libitum*. Prior to all experimental procedures, animals were anesthetized with ketamine (1mg/g weight)/medetomidine (0.02 μg/g weight). Genotypes were determined from tail extracted genomic DNA, using primers for the detection of exon 2 of TTR (which is disrupted in TTR KO by the neomycin resistance gene) and primers for the neomycin resistance gene, as previously described (Episkopou et al., 1993). All experiments were performed with the observer blinded to the animal's genotype.

Neuromuscular junction analysis

For whole muscle preparations, 24 months-old mice were killed using a lethal anesthesia dosage. Gastrocnemius muscles were dissected in PBS and fixed in 4% paraformaldehyde for 20 min, washed in PBS and incubated overnight in 0.1 M glycin at 4ºC. After permeabilization with 0.5% Triton X-100 for 15 minutes, muscles were incubated 1 h with 5μg/ml α-bungarotoxin (B-1601, Molecular Probes) in 1mg/ml BSA, washed and mounted in PBS. Images were taken using a Zeiss Axio Imager Z1 fluorescence microscope at a 20x magnification. Quantifications were performed using AxioVision (Release 4.8).

Morphometric analysis

Mice were killed using a lethal anesthesia dosage. Nerve segments with 3 mm were fixed overnight in 1.25% glutaraldehyde in 0.1 M sodium cacodylate, washed in 0.1 M sodium cacodylate for 30 min, postfixed in 1% osmium tetroxide in 0.2 M sodium

cacodylate for 60 min, washed again in 0.1M sodium cacodylate for 30 min, dehydrated using a series of graded alcohols and propylene oxide, and embedded in epon. Transverse sections (1.0 μm thick) were cut with a SuperNova, Reichest, Leica ultramicrotome, and stained with 1% toluidine blue in an 80°C heating plate for 20 s. For each animal, the total number of myelinated fibers present in one semithin section was determined by counting 40X magnified photographs covering the whole nerve area. To determine the density of unmyelinated fibers, ultrathin transverse sections were cut and stained with uranyl acetate and lead citrate. For each animal, 20 non-overlapping photomicrographs (7000X amplification) corresponding to ≈ 9000 μm^2 of each ultrathin section were taken and analyzed using a transmission electron microscope (Zeiss 902A). To assess possible differences in nerve total areas between strains, these were determined from either 4X or 10X magnified photos of sciatic nerve transverse sections using the ImageProPlus software (Infaimon, Aveiro, Portugal).

Nerve injury

Mice were anaesthetized and a 4 mm long incision was made in the shaved thigh skin. For nerve crush, the sciatic nerve was exposed and crush was performed using Pean forceps, twice during 15 s. To standardize the procedure and yield reproducible sensorimotor deficits, the crush site was maintained constant for each animal at 35 mm from the tip of the third digit. A single skin suture, immediately above the crush site, served as an additional reference. After surgery, animals were allowed to recover for 15 or 30 d after which the injury site was identified based on its position and on the presence of a subtle epineural scar.

In vivo analysis of retrograde transport using cholera toxin B

The sciatic nerve of WT and TTR KO mice was exposed and transected at the midtight level; a solution of the retrogradely transported cholera toxin B subunit (0.5 mg/ml, List Biological) was applied to the proximal end of the transected sciatic nerve for 35 min. The skin was subsequently sutured and mice were allowed to recover for 72 h, after which the L4–6 DRG were collected and fixed in 4% neutral buffered formalin. To detect retrogradely labeled sensory neurons, serial 4-μm-thick DRG sections were cut and processed for anti-cholera toxin immunohistochemistry. Briefly, sections were blocked in

blocking buffer (1% BSA and 4% fetal bovine serum in PBS) for 30 min at 37°C and incubated with anti-cholera toxin antibody (Calbiochem; 1:1000) diluted in blocking buffer overnight at 4°C. Antigen visualization was performed with the biotin-extravidin-peroxidase kit (Sigma). For each animal, to determine the percentage of retrogradely labeled sensory neurons, the total number of DRG neurons, as well as the number of labeled DRG neurons presenting visible nuclei was counted every 24 μm.

Megalin immunohistochemistry

For immunohistochemistry using the sheep anti-megalin primary antibody (1:2000, kindly provided by Dr. Pierre Verroust), antigen unmasking was done by boiling 3 X in 0.5 mM EDTA 10 mM Tris pH = 9.0 solution. Sections were blocked in blocking buffer (1% bovine serum albumin and 4% fetal bovine serum in PBS) for 30 min at 37°C and incubated with primary antibody diluted in blocking buffer overnight at 4°C. Antigen visualization was performed with the biotin-extravidin-peroxidase kit (Sigma). Slides were counterstained with hematoxylin (Merck).

Statistical analysis

Statistical analysis was performed using the Student's T-test. Results were expressed as average ± SEM.

RESULTS

Aged TTR KO mice present normal peripheral nerves and neuromuscular junctions

We investigated possible differences in the peripheral nervous system of TTR KO mice (24 months-old) when compared to WT littermates. To determine if the lower sensorimotor performance of TTR KO mice was related to altered neuromuscular junctions (NMJ), we analyzed the lower limb muscles of 24 month-old mice. No differences were observed in NMJ morphology. Also, no differences were found in the total areas of individual junctions (figure 1).

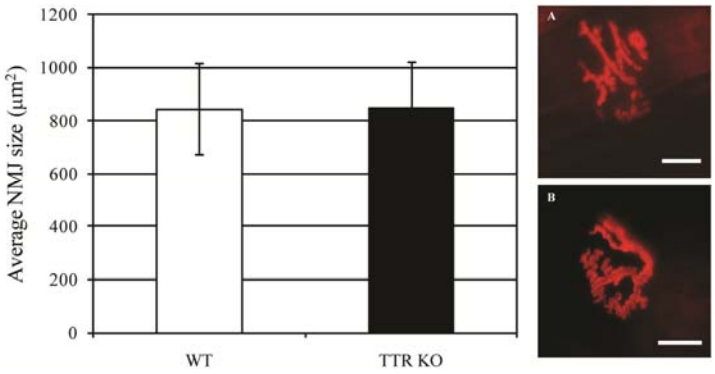

Figure 1 – TTR KO mice present normal motor-end plates. Average NMJ size (μm^2). Pictures illustrate (**A**) WT (*n* = 3) and (**B**) TTR KO (*n* = 4) NMJs stained with α-bungarotoxin-Texas Red. Scale bar = 20 μm.

Moreover, by morphometric analysis, no differences were found in peripheral nerves of old mice (figure 2).

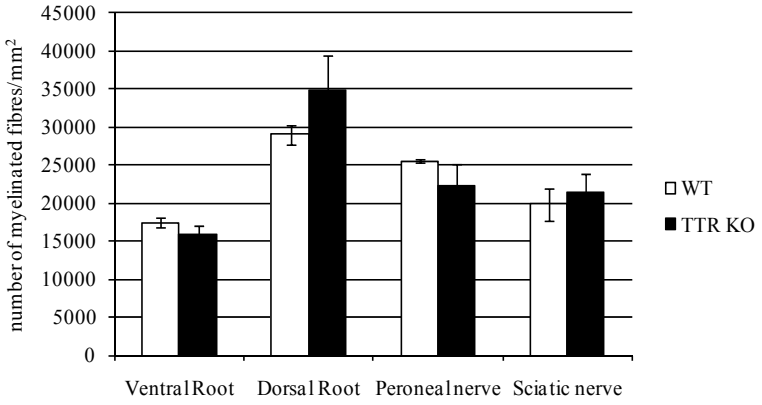

Figure 2 – Morphometric analysis of aged WT (n=3) and TTR KO (n=4) mice peripheral nerves. Results are presented as average ± SEM.

Taken together, these results suggest that the lower sensorimotor performance of TTR KO mice is not related to an altered motor-end plate conformation. However, we should not discard the hypothesis of an impairment in the terminal axons that innervate distal muscles. Further studies should address this issue.

In summary, our results show that, under physiological conditions, lack of TTR does not compromise sciatic nerve development and does not affect muscle innervation.

After sciatic nerve crush, lack of TTR is related to a decreased regeneration capacity

We raised the hypothesis that the consequences of TTR deficiency could be strengthened under stress. In fact, by functional analysis, TTR KO mice were reported as having approximately a 50% decreased motor nerve conduction velocity following nerve crush when compared to WT mice (Fleming et al., 2007). To assess whether the decreased functional performance of TTR KO mice correlated with neuropathological findings, nerve regeneration was scored by morphometry in 3, 6, and 12-months-old WT and TTR KO mice where nerve crush was performed and regeneration was assessed 15 and 30 days post-crush by morphometric analysis of the distal stumps.

TTR KO mice presented, after 15 days of regeneration, an approximately 20% decrease in the total number of myelinated fibers (figure 3A) when compared to WT littermates although, after 30 days of regeneration, no statistically significant differences were observed neither on the total number of myelinated fibers (figure 3A) nor in the g ratio (data not shown) between strains.

In relation to the density of unmyelinated fibers, after 15 days of regeneration, TTR KO mice presented a trend for a lower fiber density in all age groups, (figure 3B), whereas, after 30 days of regeneration, TTR KOs presented an approximately 40% lower density of unmyelinated fibers when compared to WT mice (figure 3B). These results were unrelated to differential nerve areas as, both after 15 and 30 days of regeneration, no differences were found between the total nerve areas of WT and TTR KO mice (data not shown).

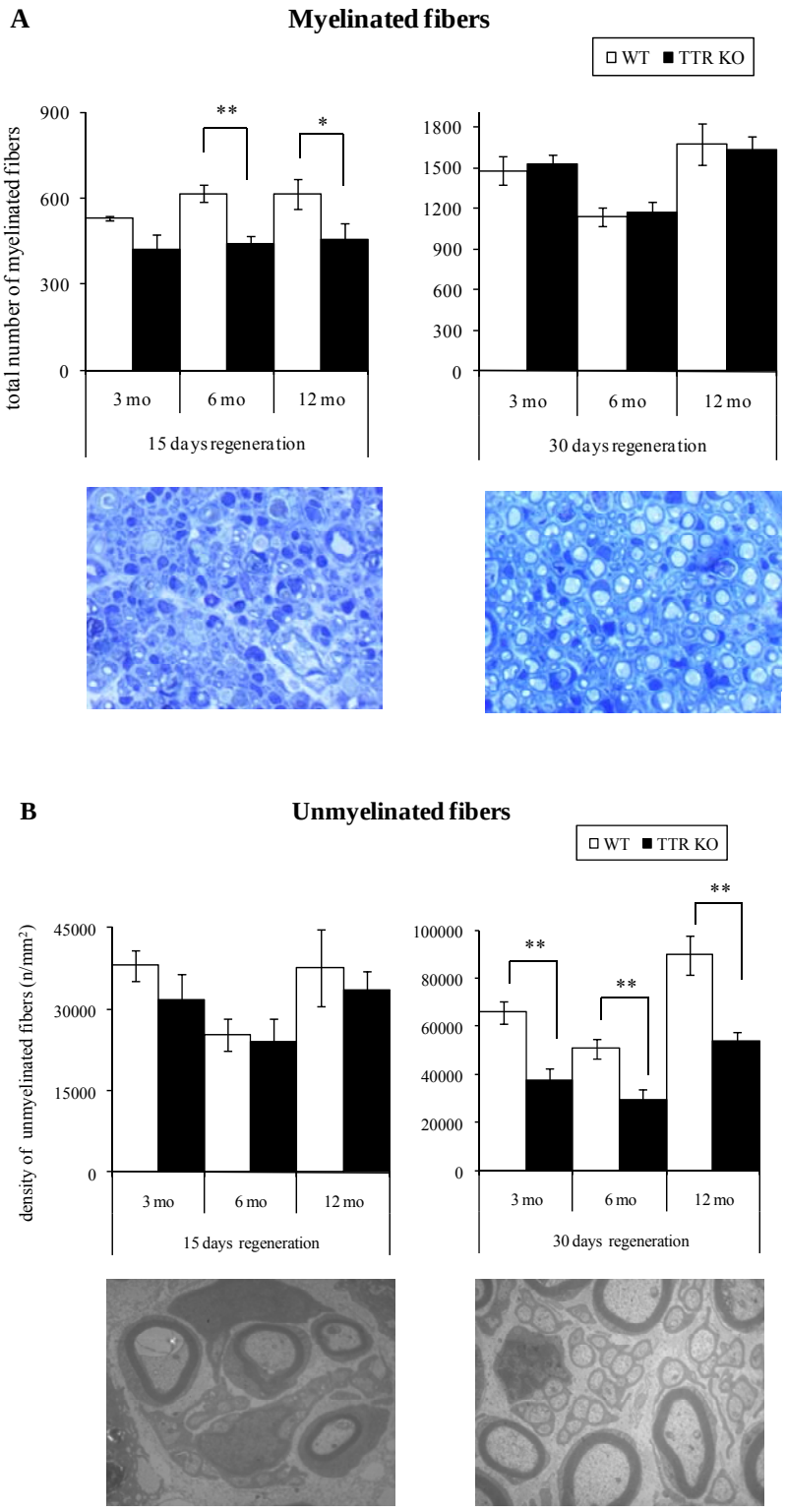

Figure 3 – Lack of TTR delays nerve regeneration. (**A**) Total number of myelinated fibers in the distal nerve segments of 3, 6, and 12-months-old WT and TTR KO mice 15 (WT: n = 4, n = 5, and n = 4; TTR KO: n = 5, n = 5, and n = 4, respectively for each age group), and 30 days (WT: n = 6, n = 5, and n = 4; TTR KO: n = 5, n = 5, and n = 6, respectively for each age group) after nerve crush; (**B**) Density of unmyelinated fibers in the distal nerve segments of 3, 6, and 12-months-old WT and TTR KO mice 15 and 30 days after nerve crush (number of animals assessed were the same as detailed in (**A**); mo- months, *$p < 0.05$, **$p < 0.01$.

In summary, our data shows that the lack of TTR delays nerve regeneration as seen morphometrically by the decrease in the number and density of myelinated and unmyelinated fibers.

Expression of TTR in the nerve of TTR KO mice leads to gain of regenerative capacity

The Thy1.2 promoter (Caroni, 1997) allows expression in both sensory and motor neurons. As such, transgenic mice expressing human TTR under the control of the Thy1.2 promoter were generated (Sousa et al., 2004c). These mice were subsequently backcrossed to a TTR KO background, resulting in a mouse strain (Thy1.2-TTRxTTR KO mice) that expresses human TTR in neurons with no expression of endogenous mouse TTR (Fleming et al., 2007).

No differences in the morphometric analysis (number of both myelinated and unmyelinated fibers) were observed comparing sciatic nerves from Thy1.2-TTRxTTR KO with nerves from WT and TTR KO mice under physiological conditions (data not shown). However, when nerve crush in Thy1.2-TTRxTTR KO mice was preformed, we observed an increase of the regenerative capacity of these mice when compared to WT and TTR KO. At 15 days of regeneration, Thy1.2-TTRxTTR KO mice showed an augment of 40% in the number of myelinated and unmyelinated fibers, respectively, in relation to WT. Furthermore, we observed an increase of 55% and 45% in the number of myelinated and unmyelinated fibers, respectively, in Thy1.2-TTRxTTR KO mice when compared the TTR KO mice (figure 4).

As expected, the three strains presented similar number of myelinated fibers after 30 days of regeneration. However, the Thy1.2-TTRxTTR KO mice (n = 6), presented a 21% increase in the density of unmyelinated fibers when compared TTR KO mice (figure 4), reinforcing the evidence of TTR's regenerative capacity.

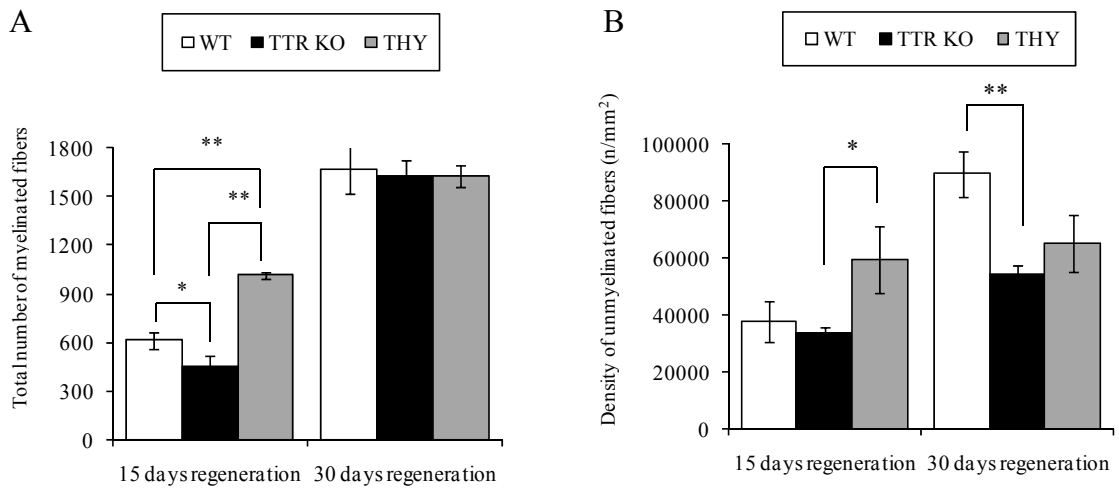

Figure 4 – Regeneration of 12-months-old WT and TTR KO mice and 18-months-old Thy1.2-TTRxTTR KO mice, 15 and 30 days after nerve crush. (**A**) Total number of myelinated fibers; (**B**) Density of unmyelinated fibers; THY-Thy1.2-TTRxTTR KO mice, * $p< 0.05$, ** $p< 0.01$.

Our results show that neuronal TTR expression in a TTR KO background increases the regenerative capacity rescuing their phenotype.

Local TTR delivery to the crushed nerve rescues the regeneration phenotype of TTR KO mice

The hypothesis that local TTR delivery to the injury site revert the phenotype of TTR KO mice was tested. After crush, human TTR fluorescently labelled with Alexa 488 (hTTR-Alexa 488) was locally administrated to the crush site. Mice were allowed to recover for either 15 or 30 days. Matrigel (the chosen vehicle composed by extracellular matrix components) is constituted by laminin which hasten nerve regeneration *in vivo* (Madison et al., 1985). One day after crush, hTTR-Alexa 488 was detected in the injury site demonstrating the effectiveness of focal administration (Fleming et al., 2009).

The lack of TTR could not be reversed by delivering to the nerve Matrigel alone as a decrease of 24% in the density of myelinated fibers was still observed in TTR KO in relation to WT mice (figure 5A and 4B). Nevertheless, following delivery of Matrigel coupled with TTR, TTR KO littermates presented a similar density of myelinated fibers to WT mice, restoring the normal phenotype (figure 5A).

In relation to unmyelinated fibers, as expected, no differences in their density were found between strains after 15 days of regeneration (Fleming et al., 2007). Therefore, the

density of unmyelinated fibers in the injured nerves supplemented with Matrigel alone or coupled with hTTR-Alexa 488 was not assessed at this time point. After 30 days of regeneration, although TTR KO nerves where Matrigel alone was delivered presented a 30% lower density of unmyelinated fibers (figure 5C), TTR KO nerves where Matrigel coupled to hTTR-Alexa 488 was added in the injury site, reached WT levels, overcoming the lack of TTR and, similary to the myelinated fibers, rescuing the WT phenotype.

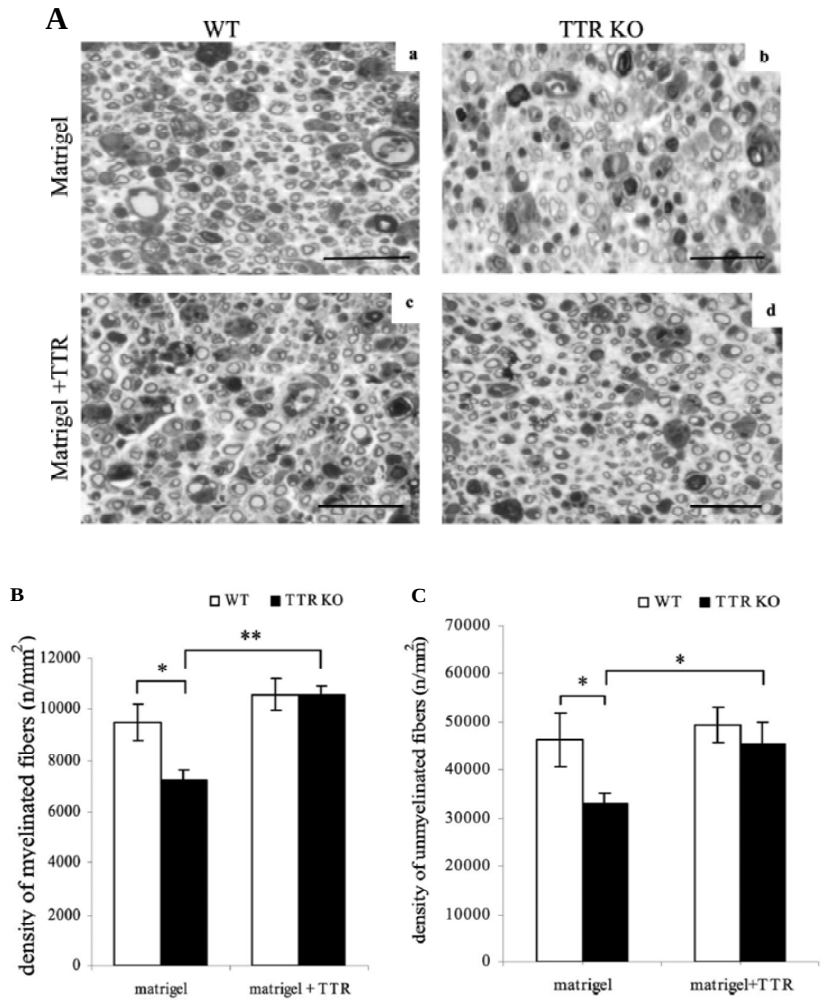

Figure 5 – Local delivery of TTR to the crushed nerve. (**A**) Semithin sections of distal nerve stumps 15 d after nerve crush from WT mice (**a**, **c**) and TTR KO mice (**b**, **d**), in which Matrigel either alone (**a**, **b**) or supplemented with TTR (**c**, **d**) was added. Scale bars = 10 μm. (**B**) Corresponding density of myelinated fibers. WT: n=6 and n= 7; TTR KO: n=5 and n=7, respectively, for each setting. (**C**) Density of unmyelinated fibers 30 d after nerve crush in WT and TTR KO mice, in which Matrigel either alone or supplemented with TTR was added. WT: n=6 and n=5; TTR KO: n=8 and n=8, respectively, for each setting; Matrigel alone (matrigel), Matrigel supplemented with TTR (matrigel-TTR).*$p<0.05$, **$p<0.01$.

In summary, our data shows that local TTR delivery to the crush site rescues the regenerative impairment of TTR KO mice further reinforcing the observation that TTR is a regeneration enhancer.

TTR KO mice present a compromised retrograde transport

In order to determine the reason for the impaired regenerative capacity of TTR KO mice, retrograde transport was analysed.

$p75^{NTR}$ is a receptor that undergoes retrograde transport after binding neurotrophins at the axonal terminals (Curtis et al., 1995) and, as it accumulates in the distal side on ligated nerves, it is a good tool to evaluate retrograde transport (Johnson et al., 1987; Taniuchi et al., 1988). TTR KO mice presented compromised retrograde transport as they were described as having accumulation of $p75^{NTR}$ in the distal side on ligated nerves after chronic constriction injury, despite no differences were detected in the $p75^{NTR}$ expression between WT and TTR KO nerves (Fleming et al., 2009).

To further establish, *in vivo*, the relation between the absence of TTR and the impairment of retrograde transport, WT (n = 6) and TTR KO (n = 5) sciatic nerves were retrogradely labelled with cholera toxin B. The DRG neurons of TTR KO mice presented an approximately 30% lower number of cells labelled with cholera toxin when compared to WT littermates (figure 6), corroborating the previous results.

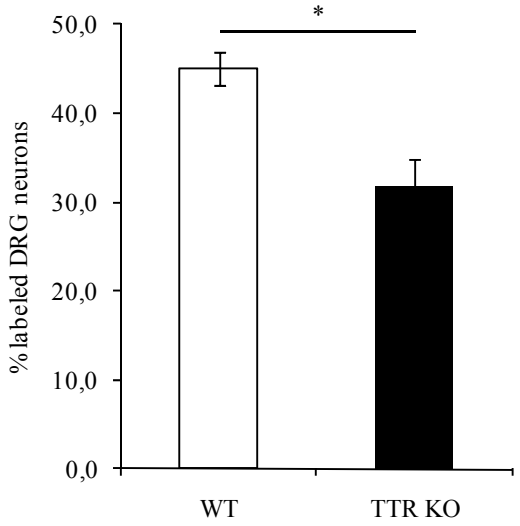

Figure 6 – TTR KO mice present a lower number of DRG neurons labelled with cholera-toxin when compared to WT DRG neurons following retrograde transport with cholera toxin B. *p < 0.05

These data suggest that the TTR KO lower regenerative capacity may be delayed due to a compromised retrograde transport.

Megalin is expressed by DRG neurons and is necessary for TTR neuritogenic effect

Megalin is an endocytic TTR receptor well described in the kidney (Sousa et al., 2000) and is implicated in metallothionein uptake by neurons (Ambjorn et al., 2008; Fitzgerald et al., 2007). As this receptor could be the key to understand TTR uptake by neurons (Fleming et al., 2009) needed for the neuritogenic activity of this protein, we verified if DRG neurons were able to express megalin. By immunohistochemistry (and using kidney as a positive control) we confirmed that, in fact, DRG neurons express megalin (figure 7). These results corroborate previous data where megalin expression was confirmed by RT-PCR (Fleming et al., 2009).

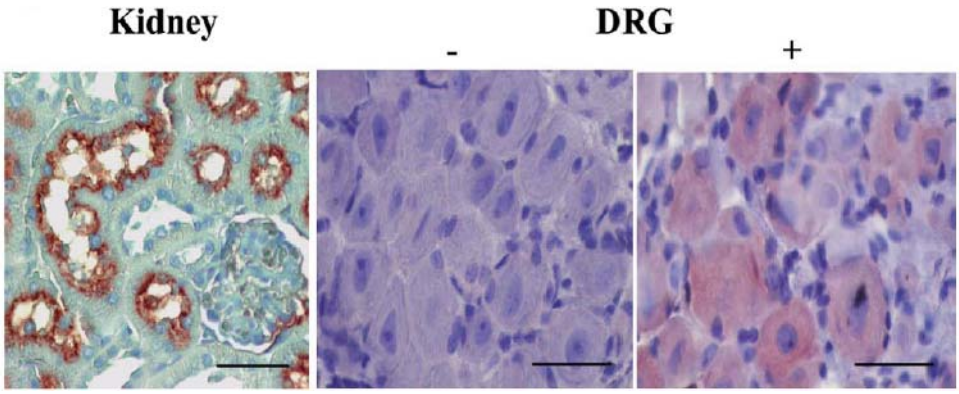

Figure 7 – TTR internalization by DRG neurons is megalin mediated. Megalin immunohistochemistry of kidney (left), and DRG in the absence (–, middle) and presence (+, right) of primary antibody. Scale bar = 50 μm.

In vivo, decreased megalin levels lead to decreased nerve regeneration in a TTR-dependent process

Nerve crush was performed in WT, TTR KO, megalin heterozygous (MEG (+/-)) – we used megalin heterozygous as homozygous animals died minutes after birth (Willnow et al., 1996) – and TTR KO/MEG (+/-) animals to evaluate the influence of megalin in the action of TTR *in vivo*. After 15 days of recovery, sciatic nerve was collected and assessed by morphometry. According to previous results, TTR KO mice showed a decrease (30 %) in the density of myelinated fibers. TTR KO/MEG (+/-) and MEG (+/-) mice had similar results suggesting that, in nerve regeneration, there is no influence of other megalin ligands

and that megalin plays an important role in the process of sciatic nerve regeneration (figure 8).

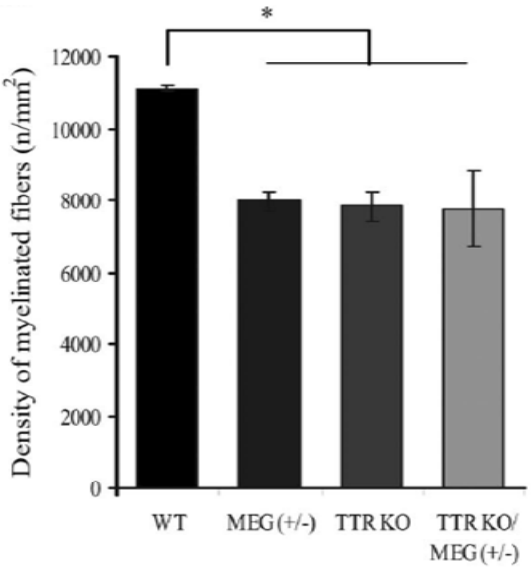

Figure 8 – Morphometric analysis of sciatic nerves from WT, TTR KO, MEG (+/-), and TTR KO/MEG (+/-) mice. Density of myelinated fibers 15 days after nerve crush. *$p < 0.05$.

In summary, TTR internalization by sensory neurons is megalin mediated and necessary to promote nerve regeneration.

DISCUSSION

The neuromuscular junction (NMJ) is the sole communicative link between motorneurons and muscle fibers. Its structure and function is reviewed by Hirsch (2007). The cause for the sensorimotor impairment in TTR KO mice still needs to be disclosed as, under physiological conditions, no differences were found in the areas of NMJs nor in the density of myelinated and unmyelinated fibers in the sciatic nerve of TTR KO mice when compared to WT littermates. In addition, the motor discoordination was not related to differences in the cerebellum (Fleming et al., 2007). However, this impairment can be related to motor neuron death or defects in terminal axons. Further studies should evaluate if motor axon abnormalities such as axonal swellings, demyelinated axonal segments or extensive axons branching (Court et al., 2008) are causing this impairment. Preliminary analysis of TTR KO and WT mice sciatic nerve microarrays suggest a downregulation in genes encoding cytoskeleton structures, namely, specific proteins of intermediate filaments in the nervous system. The downregulation of genes such as those encoding neurofilament, contactin and tau (9-fold, 6-fold and 3-fold respectively) can be related to an impairment in the axonal cytoskeleton and, consequently, be the cause of motor discoordination.

Nerve regeneration is a process of the utmost importance in biological systems. Although the PNS has a regeneration permissive environment, as axons sprout in adult peripheral nerves after injury, target innervation is often incomplete, resulting in a disappointing functional recovery. The functional and morphometric analysis here described clearly demonstrates that TTR enhances and accelerates regeneration; in the scenario of nerve regeneration, timely target innervation is crucial for regain of functional capacity. In relation to unmyelinated fibers, the absence of differences in their number after 15 days of regeneration, might be due to the impossibility at this time point to clearly distinguish fibers that will become small myelinated axons from those that will in fact remain unmyelinated; TTR is therefore probably related to a decreased number of unmyelinated fibers throughout the whole regeneration process. These results suggest that the absence of TTR is related to a delayed axonal growth of myelinated fibers, as reflected by their decreased number after 15 days of regeneration that, however, reaches WT numbers after 30 days of regeneration.

The impact of TTR in nerve regeneration was further established through the demonstration that either genetic correction or local TTR delivery was successful in

abolishing the differences between WT and TTR KO mice. When an injury takes place, plasma TTR has its entrance in the nervous tissue facilitated, as the BNB is disrupted. In recipients of FAP livers, TTR deposits were found within the nerve, suggesting that plasma TTR can cross the BNB (Sousa et al., 2004b). Intravenous injection of hTTR-Alexa 488 show that plasma TTR is, in fact, able to enter intact nerves through the BNB (Fleming et al., 2009), which is effective in slowing but not in preventing the entry of proteins into the endoneurium (Wadhwani and Rapoport, 1994). Local TTR expression in the nerve rescued the TTR KO slower regenerative phenotype in Thy1.2-TTRxTTR KO mice. The faster regeneration of Thy1.2-TTRxTTR KO mice in relation to WT animals was probably due to the fact that TTR expression in neurons is not a physiological situation; under normal conditions, as occurs in WT mice, TTR might enter the endoneurium through the blood and CSF, whereas Thy1.2-TTRxTTR KO express TTR locally in 70% of all sensory and motor neurons (Sousa et al., 2004c).

One should note that in regeneration, TTR effect probably does not result from impaired retinoic acid or thyroid hormone metabolism as, despite low plasma retinol levels, TTR KO mice are euthyroid (normal thyroid gland function) (Palha et al., 1994) and do not show any symptoms of vitamin A deficiency (Episkopou et al., 1993).

Additionally to a decreased axonal growth, TTR KO axons have lower levels of retrograde transport both *in vitro* and *in vivo*. Being the transmission of signals to the cell body a key process in nerve regeneration, the compromised retrograde transport of TTR KO axons might be, at least in part, responsible for the delayed regenerative capacity of TTR KO mice and decreased neurite outgrowth in the absence of TTR. TTR internalization by a clathrin-dependent endocytic process is crucial for the enhancement of neurite outgrowth by TTR as, when the protein was prevented from being internalized, neurite outgrowth was abolished (Fleming et al., 2009). Megalin, an endocytic TTR receptor (Sousa et al., 2000), is involved in receptor-mediated endocytosis in clathrin-coated pits of a wide range of ligands and was described as being important for preventing TTR filtration through the glomerulus (Sousa et al., 2000). In addition to megalin expression in DRG neurons, our results show that decreased levels of megalin lead to decreased nerve regeneration and that TTR neuritogenic activity depends on its internalization by this receptor. Also, the relevance of megalin in the nerve is supported by the fact that its partial absence is sufficient to impair TTR-mediated enhancement of nerve regeneration further

validating the importance of this receptor in the nervous system and particularly in the course of nerve regeneration.

In conclusion, the presence of TTR in the nerve, and its internalization by megalin receptors in the DRG, is a key factor in a timely effective response to promote nerve regeneration after injury. As such, TTR promotes a correct axonal outgrowth that is crucial for correct target innervation.

CHAPTER II

Assessment of the biological consequences of the increased NPY levels in TTR KO mice

INTRODUCTION

Transthyretin (TTR) KO mice show increased levels of amidated neuropeptides due to overexpression of peptidylglycine α-amidating monooxygenase (PAM) (Nunes et al., 2006), the only enzyme that α-amidates peptides, which is rate-limiting in the process of neuropeptide maturation, as its substrates exist in excess (Mains et al., 1987; Prigge et al., 2000). Among the neuropeptides which are amidated by PAM, neuropeptide Y (NPY) is the most abundant both in the central and peripheral nervous system. As NPY requires PAM-mediated α-amidation for biological activity (Eipper et al., 1992) PAM overexpression in TTR KO mice results in increased levels of processed amidated NPY, without an increase of NPY expression (Nunes et al., 2006). TTR KO mice show a significant NPY-overexpressor phenotype including a decreased body temperature, an increased carbohydrate preference and consumption (Nunes et al., 2006) and reduced depressive behavior (Sousa et al., 2004a).

NPY has been correlated with alterations in bone mass although controversy still surrounds this issue. A recent study revealed that exogenous NPY administration does not produce any alteration in cancellous bone mass (Allison et al., 2009; Baldock et al., 2002). However, a decrease in bone mass after NPY intracerebroventricular infusion has already been reported (Ducy et al., 2000). As NPY action in the bone is still controversial and given that TTR KO mice are a mouse model for increased NPY, studies were preformed to evaluate whether, similarly to the nervous system, increased NPY levels were found in bones of TTR KO mice. Nunes et al (2009a) reported that NPY expression was detected in various adult bone cells and, as expected, with higher levels in TTR KO mice. Increased alkaline phosphatase activity and osteocalcin expression in TTR KO bone marrow stromal cells suggested an enhanced competence to undergo osteoblast differentiation (Nunes et al., 2009a).

In this study we further investigate the biological consequences related to the increased NPY levels associated with increased PAM expression in bone of this strain.

Accumulating evidence shows a neuroprotective action of NPY, as well as a stimulating effect on neurogenesis leading to an increased proliferation of adult neuronal precursor cells in the dentate gyrus (DG) (Howell et al., 2005) and subventricular zone (Agasse et al., 2008). Recently, Nunes et al (2009b) reported that TTR KO mice organotypic hipocampal slice cultures display decreased AMPA–induced

neurodegeneration. Taken together, it is plausible that the increased NPY levels in the hippocampus of TTR KO mice (Nunes et al., 2006) are responsible for the neuroprotection in TTR KO hippocampal cultures, as NPY prevents neuronal cell death in organotypic hippocampal slice cultures exposed to an excitotoxic insult (Silva et al., 2003; Xapelli et al., 2007). In this respect, we addressed the effect in neuroproliferation of increased NPY levels in TTR KO mice.

MATERIALS AND METHODS

Animals

Mice were handled according to the European Communities Council Directive (86/609/EEC) as well as to the National rules and all studies performed were approved by the Portuguese General Veterinarian Board. WT and TTR KO littermate mice were obtained from the offspring of heterozygous breeding pairs and maintained at 24 ± 1^{o}C under a 12 h light/dark cycle and fed regular chow and tap water *ad libitum*. Prior to all experimental procedures, animals were anesthetized with ketamine (1mg/g weight)/medetomidine (0.02 μg/g weight).

Bone Histology

Femurs were harvested from 3 month old male WT (n=6) and TTR KO (n=5) mice. After measuring their length, bones were fixed in 4% paraformaldehyde in PBS, decalcified as described above and embedded in paraffin. Serial 10-um-thick longitudinal sections were cut. Sections were then deparaffinated, dehydrated in a modified alcohol series and stained for hematoxilin/eosin.

Immunohistochemistry

Femurs from 3 month old male WT (n=6) and TTR KO (n=5) littermates were fixed in 4% paraformaldehyde in PBS, decalcified in TBD-1 commercial solution (Thermo Electron Corporation), embedded in paraffin, and serial 4-μm-thick longitudinal sections were cut. For studies during embryonic development, 16 or 18 days WT pregnant females were killed by cervical dislocation, and the fetuses were collected by cesarian section. Sections were then deparaffinated, dehydrated in a modified alcohol series and blocked for the endogenous peroxidase activity. NPY immunohistochemistry was performed with the MOM Kit (Vector), following the manufacturer's instructions. Briefly, bone sections from WT and TTR KO mice, were incubated in the MOM kit blocking reagent for 1 hour at room temperature, prior to incubation with the monoclonal NPY antibody, NPY05 (generously provided by Dr. Eric Grouzmann, University Hospital, Lausanne, Switzerland, 1:2,000 in MOM diluent) for 1 hour at room temperature. NPY05 is specific for the amidated form of NPY (Grouzmann et al., 1992). Antigen visualization was performed

with the MOM Avidin:Biotinylated peroxidase Complex (ABC) reagent (Vector), using 3-amino-9-ethyl carbazole (Sigma) as substrate. On parallel control sections, the primary antibody was replaced by mouse immunoglobulin G (Sigma). Immunohistochemistry for osteocalcin (a positive control for osteoblast staining) and PAM were also performed. Briefly, sections were incubated in blocking buffer (1% BSA, and 4% bovine serum in PBS) for 30 min at 37ºC in a moist chamber, followed by the incubation with primary antibodies at the appropriate dilution in blocking buffer, overnight at 4ºC. The dilutions used were 1:500 for goat anti-osteocalcin (Biomedical Technologies Inc) and 1:500 for rabbit anti-PAM (kindly provided by Dr Richard Mains, University of Connecticut Health Center). Antigen visualization was performed with the biotin-extravidin-peroxidase kit (Sigma), using 3-amino-9-ethyl carbazole (Sigma) as substrate. On parallel control sections, the primary antibody was replaced by blocking buffer. Immunohistochemistry analysis was carried out independently by two observers. For quantification of PAM immunohistochemistry, the number of labeled cells/mm^2 was scored in 3 non-overlapping micrographs with a magnification of 40x.

Bone marrow stromal cell culture

Primary BMSCs were obtained according to the method developed by Maniatopoulos et al (Maniatopoulos et al., 1988). Briefly, femurs and tibias from 1 month old male WT and TTR KO littermates were aseptically excised from the hind limbs, the epiphyses cut off, and the marrow flushed with standard culture medium, which consisted of alpha-MEM supplemented with 10% FBS, 50 μg/mL gentamicin sulfate, and 2.5 μg/mL amphotericin B (Invitrogen). Cells were seeded in 75-cm^2 plastic culture flasks, and incubated in a humidified incubator (37°C and 5% CO_2). The medium was changed after the first 24 h to remove nonadherent cells. Subsequently, the adherent cells were cultured for 10 days, the medium being renewed every 3 days.

Differentiated bone marrow stromal cells

BMSCs were cultured as above, trypsinized and seeded in 24-well plates at a density of $4x10^4$ cells per well. Cells were then differentiated in osteoblasts by the addition of 50 μg/mL Vitamin C (Sigma) and 10 mM beta-glycerophosphate (Sigma) to the culture medium, and cultured for 3, 7 and 14 days.

Reverse transcription-PCR

Total RNA from cell culture samples was isolated with the RNeasy Micro Kit (Qiagen) and subjected to RT-PCR with the Superscript II kit (Invitrogen). PCR was performed for the appropriate number of cycles for each cDNA (20-40 cycles) at 95ºC for 1 min, 56ºC for 2 min and 72ºC for 3 min. Sense and antisense primers were:

- for β-actin:
  - 5'-GTGGGCCGCTCTAGGCACCAA-3' and
  - 5'-CTCTTTGATGTCACGCACGATTTC-3';
- for HPRT:
  - 5'-GTAATGATCAGTCAACGGGGGAC-3' and
  - 5'-CCAGCAAGCTTGCAACCTTAACCA-3';
- for GAPDH:
  - 5'-ACTCCACTCACGGCAAATTC-3' and
  - 5'-CCTTCCACAATGCCAAAGTT-3';
- for NPY:
  - 5'-TGGACTGACCCTCGCTCTAT-3' and
  - 5'-GATGAGGGTGGAAACTTGGA-3';
- for osteocalcin:
  - 5'- CTCTGTCTCTCTGACCTCACAG-3' and
  - 5'-CAGGTCCTAAATAGTGATACCG-3' (Salingcarnboriboon et al., 2006);
- for osteopontin:
  - 5'-TCTGATGAGACCGTCACTGC-3' and
  - 5'- TCTCCTGGCTCTCTTTGGAA-3';
- for PAM:
  - 5'-CCTGGGGTCACACCTAAAGA-3' and
  - 5'-TGTAAGGACACACCGGAACA-3';

Unreferenced primers were designed using PRIMER3 (http://frodo.wi.mit.edu/cgi-bin/primer3/primer3_www.cgi) and the sequence from the National Centre for Biotechnology Information database. All primers used were located on two different exons to ensure that only properly spliced mRNA and not genomic DNA contaminants was amplified. Ethidium bromide-stained gels were scanned using a Typhoon 8600 (Amersham) and amplified bands were quantified using the ImageQuant software (Amersham). Fluorescence density of each PCR-amplified band was normalized with the corresponding value of β-actin, HPRT and/or GAPDH. Experiments were made in triplicate and a representative amplification is shown.

BrdU treatment and immunohistochemistry

Three-month old male WT (n=6) and TTR KO (n=6) mice were injected i.p. with 50 mg/kg BrdU once a day for 3 consecutive days. Twenty-four hours after the last injection, animals were perfused with 4% paraformaldehyde, 4% sucrose and 0.9% NaCl pH 7.4. Brains were paraffin-embedded and serial 4-µm-thick coronal sections were cut through the forebrain at levels including the lateral ventricles and the hippocampus with 6 sections (spaced between each other by 60 µm) mounted per slide. BrdU immunohistochemistry was performed using monoclonal BrdU antibody (1:1,000 in MOM diluent). For each animal, BrdU-immunoreactive cells in the DG and SVZ were counted bilaterally on 3 consecutive slides. To control BrdU treatment and immunohistochemistry, the small intestine (which contains numerous rapidly proliferating cells) of each of the analysed mice, was processed similarly for BrDU immunohistochemistry.

Statistical analysis

Statistical analysis was performed using the Student's T-test. Results were expressed as average ± SEM.

RESULTS

TTR KO bone presents higher levels of PAM and NPY expression

We determined that NPY expression in bone starts early at day 16 of embryonic development in megakaryocytes, articular chondrocytes and osteocytes (figure 1). Moreover, it was shown by our group that NPY is expressed in the same cell types in the adult bone and that TTR KO mice have an increased content of amidated NPY in the bone when compared to WT littermates (Nunes et al., 2009a).

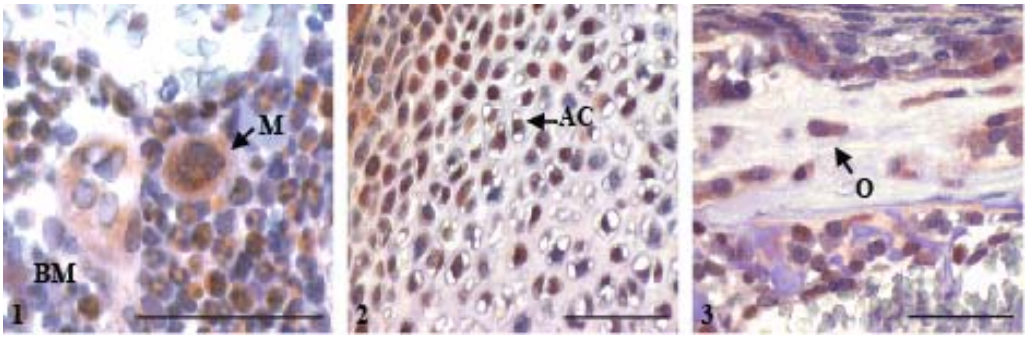

Figure 1 – NPY-immunoreativity detected in bone embryos at day 16 of development. Panel 1 – megakaryocyte (M) and bone marrow (BM); panel 2 – articular chondrocytes (AC); panel 3 – osteocyte (O). Scale bar = 50 μm.

Since increased PAM expression was observed both in the PNS and CNS of TTR KO mice underlying the increased NPY levels in the nervous system (Nunes et al., 2006), we hypothesized that the increased levels of NPY detected in the bone of TTR KO mice were related to increased PAM expression in this tissue. In fact, PAM-immunoreactivity was detected in megakaryocytes and other various bone cell types (figure 2A). Moreover, by densitometry, TTR KO littermates presented a higher number of bone marrow cells labelled with α-PAM antibody per mm^2 when compared to WT (figure 2B).

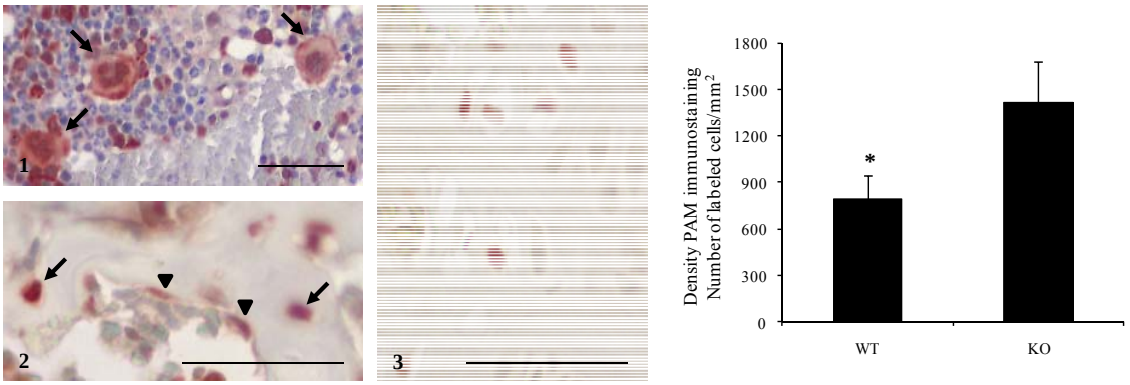

Figure 2 – PAM is expressed in bone. (**A**) PAM-immunoreactivity is detected in megakaryocytes (panel 1, arrows), osteocytes (panel 2, arrows), osteoblasts (panel 2, arrowheads) and chondrocytes (panel 3). Scale bar = 50 µm. (**B**) Quantification of the density of PAM immunostaining in the bone marrow of WT and TTR KO mice. *p<0.05.

Increased NPY in the bone of TTR KO mice is related to increased osteoblastic differentiation

We analyzed bone marrow stromal cells (BMSC) to investigate if, *in vitro*, during the course of BMSC differentiation (after 3, 7 and 14 days of culture) these differences between strains were maintained. Again, increased levels of PAM expression were observed by RT-PCR in TTR KO BMSC at day 3 and day 14 of culture when compared to WT (figure 3). These results are in accordance with the higher levels of NPY described in TTR KO BMSC during osteoblast differentiation (Nunes et al., 2009a) suggesting a putative role of NPY in osteoblast differentiation.

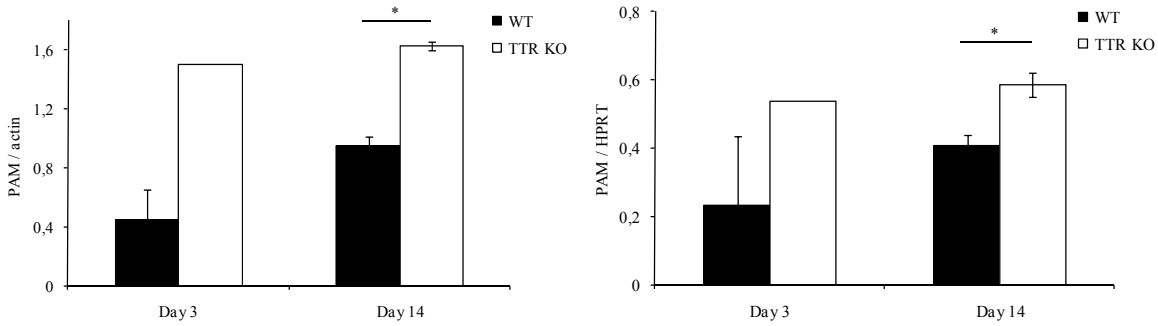

Figure 3 – PAM expression in bone cells from WT and TTR KO mice. Semiquantitative RT-PCR analysis of PAM expression normalized for actin (**A**) or HPRT (**B**) expression in BMSCs from WT and TTR KO mice at days 3 and 14 of osteoblast differentiation. Results are presented as average ± SEM; *p<0.05.

We observed increased levels of osteoblast phenotype markers namely osteopontin and osteocalcin (figure 4A and B, respectively) in TTR KO BMSC cultures.

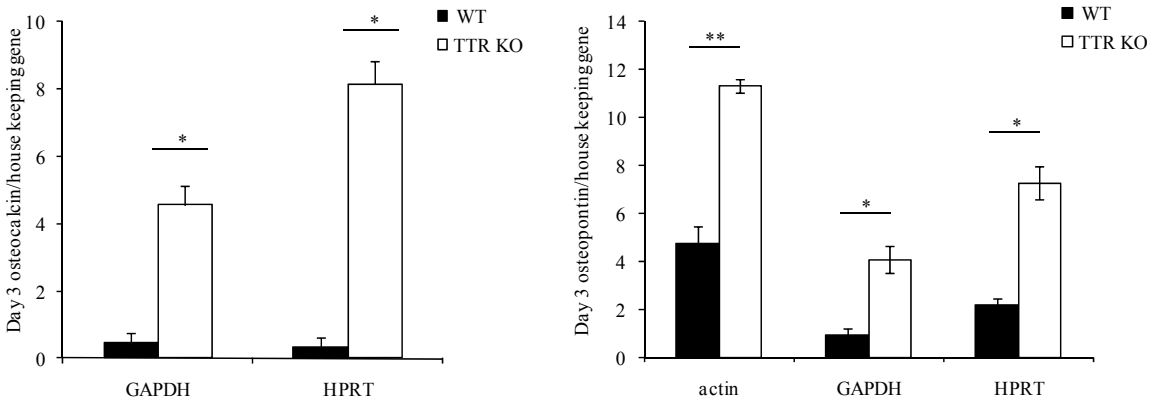

Figure 4 – Osteoblast differentiation of WT and TTR KO BMSCs as assessed by osteocalcin and osteopontin levels. Osteocalcin expression normalized for the expression of GAPDH and HPRT at day 3 (left). Osteopontin expression normalized for the expression of actin, GAPDH and HPRT at day 3 under osteoblast differentiation conditions (right). Results are presented as average ± SEM; *p<0.05; **p<0.005.

In summary, our data shows that TTR KO mice have increased PAM expression in the bone and, consequently, higher NPY levels. Moreover, our data suggest that increased NPY levels are related to the increased osteoblast differentiation.

Neuroproliferation is not affected in TTR KO brain

NPY has been described as a neuroproliferator in the *dentate gyrus* (DG) (Howell et al., 2005) and subventricular zone (SVZ) (Agasse et al., 2008). Since TTR KO mice have increased levels of neuropeptide Y and, given that neuroproliferation is one crucial factor to prevent and/or overcome neurodegeneration, the effect of TTR on the hippocampus and SVZ was assessed. The number of proliferating cells in the hippocampal DG was not different between WT and TTR KO littermates (Nunes et al., 2009b) a similar result was observed in the SVZ regarding the proliferative cell population. To control for the quality of the BrdU staining using our protocol, the small intestine of each mice was processed similarly for BrdU immunohistochemistry. In all the animals analysed, numerous rapidly proliferating cells were observerd (figure 5).

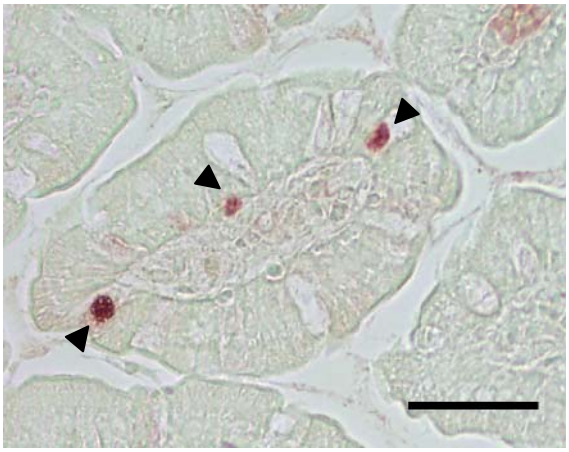

Figure 5 – BrdU immunohistochemistry in mouse intestine cells. Photomicrographs of BrdU-positive cells in intestinal cells (arrows). Scale bar = 50 μm.

In summary, despite their high levels of NPY in the brain, TTR KO mice do not display increased neuroproliferation.

DISCUSSION

NPY role in the control of bone mass is not consensual. Until now, NPY expression was only detected in bone marrow cells, including megakaryocytes (Ericsson et al., 1987). Our results show that PAM, as well as NPY, are expressed both in BMSCs and BMSCs undergoing osteoblastic differentiation (Nunes et al., 2009a). Moreover, our work also shows PAM expression in megakaryocytes, chondrocytes, osteoblasts and osteocytes.

Nunes et al. (2009a) demonstrated that TTR KO bone tissue displays increased amidated NPY levels, when compared to WT, further validating the expression of this neuropeptide in bone cells. In theoretical terms, the major TTR ligands, T_4 and retinol could be responsible, at least in part, for the bone phenotype observed in TTR KO mice. Retinol deficiency is known to increase bone mineral density (Navia and Harris, 1980); additionally, retinoic acid inhibits osteogenic differentiation of bone marrow stromal cells (Takahashi et al., 2008; Wang et al., 2008). Despite the fact that TTR KO mice have retinol plasma levels below the level of detection (Grouzmann et al., 1992), symptoms of vitamin A deficiency are absent in these animals. In agreement, their total retinol tissue levels are not significantly different from WT mice (Wei et al., 1995). Moreover, retinoic acid plasma levels are 2-3-fold higher in TTR KO mice, probably compensating their low retinol levels (Wei et al., 1995). Taking the above into account, it is highly unlikely that having normal retinol levels in tissues and increased retinoic acid in the plasma, an impairment in retinol homeostasis would be responsible for the increased bone mineral density in TTR KO mice. Regarding thyroid hormones, it is well described that hyperthyroidism in adult patients leads to decreased bone mineral density (Karga et al., 2004). As expected, both total T_4 and T_3 serum levels are decreased in TTR KO mice (Episkopou et al., 1993; Grouzmann et al., 1992). However, similarly to what is described above for retinol, this decrease is unrelated to symptoms of hypothyroidism or thyroid gland abnormalities (Palha et al., 1994). Again, in terms of tissue content, TTR KO mice present no differences in T_4 levels when compared to WT mice (Palha et al., 2000; Palha et al., 1997), probably given the high free T_4 serum pool in the TTR KOs (Palha et al., 1994), which might explain their euthyroid status. Such an euthyroid status is essential for normal skeletal development and maintenance and therefore it is hard to envisage that the bone phenotype of TTR KO mice would be related to thyroid hormones.

It is additionally possible that in TTR KO mice, as a consequence of PAM overexpression, increased levels of other amidated neuropeptides may produce some complexity. In this respect, although contradictory results have been reported for the action in bone of some amidated neuropeptides, such as substance P, others, such as pancreatic polypeptide and calcitonin gene-related peptide have been described as stimulating the differentiation of an osteoblastic cell line (Kingery et al., 2003) or increasing the number of bone colonies formed from MSC *in vitro* (Hosaka et al., 2008), similarly to what is here reported in the absence of TTR.

It is noteworthy that the increased NPY levels in TTR KOs are unrelated to increased NPY mRNA expression and result from increased processing and amidation by PAM, which is upregulated in TTR KO animals. In fact, although TTR is not expressed in BMSCs, PAM expression is increased in TTR KO BMSCs, suggesting that TTR KO osteoblasts display an intrinsic augmented PAM expression in relation to WT cells, as a consequence of their physiological TTR-free environment. A similar finding was reported in TTR KO neurons (similarly to BMSCs, neurons lack TTR expression) as these cells were also shown to display an intrinsic decreased neurite outgrowth, as a consequence of their physiological TTR-free environment (Fleming et al., 2007).

TTR KO mice, an additional model displaying increased NPY levels, have an increased cancellous bone mass phenotype (Nunes et al., 2009a) in agreement with the NPY Y2 receptor KO mice and mice lacking leptin, further suggesting that increased NPY content might be related to increased cancellous bone mass. Despite all the concerns discussed above as to the use of TTR KO mice as a model of increased NPY, the big advantage of these animals over other NPY overexpressor models is that, in addition to the increased NPY levels, leptin is not altered (Marques et al., 2007), excluding its interference in the bone phenotype observed.

Based on our observations, and given the neuroproliferative role of NPY (Hansel et al., 2001; Howell et al., 2005), the increased NPY levels observed in TTR KO mice are not related to an increase in the number of proliferating cells in the SVZ, as previously reported (Richardson et al., 2007) nor in the hippocampus. In this respect, it is possible that, in addition to the increased amidated NPY levels detected in the CSF and hippocampus of TTR KO mice, other systems are also changed, which could introduce some complexity and mask NPY proliferative effect.

In summary, our findings provide evidence that increased NPY expression in bone cells is related to increased levels of PAM expression and regulation of osteoblastic differentiation. Moreover, TTR KO mice, displaying a NPY overexpressor phenotype, present increased bone mass phenotype. However, in this model, no increase in neuroproliferating cells was observed suggesting that the neuroproliferative role of NPY should be regarded with caution.

CONCLUSIONS

CONCLUSIONS

In this work we aimed to identify a putative role for TTR in the biology of the peripheral nerve and bone. Although TTR KO sciatic nerves were similar to WT under physiological conditions, the lack of TTR was related to compromised retrograde transport and lead to a delay in nerve regeneration after injury. This phenotype could be reversed either with direct delivery of TTR (in a laminin-containing gel) or with local TTR expression in the nerve (in the Thy1.2-TTRxTTR KO mice). In the present work we did not find differences in the neuromuscular junctions of TTR KO mice that could underlie their sensorimotor impairment, suggesting that the motor discoordination of TTR KO mice might be related to molecular mechanisms not yet disclosed. To investigate the mechanism leading to a slower regeneration of TTR KO mice, the involvement of megalin, a receptor implicated in the internalization of TTR in the nerve, was investigated. *In vivo*, megalin-mediated TTR uptake was shown to be necessary for TTR activity as a regeneration enhancer.

Associated to the lack of TTR, TTR KO mice present increased PAM and NPY levels both in the sciatic nerve and bone. The higher expression of this enzyme and neuropeptide content in various bone cells is related to an increase in bone mass, as a consequence of the higher levels detected during osteoblast differentiation. In this model, we did not detect an increase in neuroproliferating cells, despite the neuroproliferative role of NPY.

In conclusion, this work contributed to clarify the role of TTR in peripheral nerve regeneration and the consequences of TTR involvement in neuropeptide maturation in the bone and brain.

REFERENCES

REFERENCES

Agasse F, Bernardino L, Kristiansen H, Christiansen SH, Ferreira R, Silva B, et al. Neuropeptide Y promotes neurogenesis in murine subventricular zone. Stem Cells 2008; 26: 1636-45.

Aleshire SL, Bradley CA, Richardson LD, Parl FF. Localization of human prealbumin in choroid plexus epithelium. J Histochem Cytochem 1983; 31: 608-12.

Allison SJ, Baldock PA, Enriquez RF, Lin E, During M, Gardiner EM, et al. Critical interplay between neuropeptide Y and sex steroid pathways in bone and adipose tissue homeostasis. J Bone Miner Res 2009; 24: 294-304.

Ambjorn M, Asmussen JW, Lindstam M, Gotfiyd K, Jacobsen C, Kiselyov VV, et al. Metallothionein and a peptide modeled after metallothionein, EmtinB, induce neuronal differentiation and survival through binding to receptors of the low-density lipoprotein receptor family. Journal of Neurochemistry 2008; 104: 21-37.

Andrade C. A peculiar form of peripheral neuropathy; familiar atypical generalized amyloidosis with special involvement of the peripheral nerves. Brain 1952; 75: 408-27.

Baldock PA, Sainsbury A, Couzens M, Enriquez RF, Thomas GP, Gardiner EM, et al. Hypothalamic Y2 receptors regulate bone formation. J Clin Invest 2002; 109: 915-21.

Blake CC, Geisow MJ, Oatley SJ, Rerat B, Rerat C. Structure of prealbumin: secondary, tertiary and quaternary interactions determined by Fourier refinement at 1.8 A. J Mol Biol 1978; 121: 339-56.

Blake CC, Geisow MJ, Swan ID, Rerat C, Rerat B. Strjcture of human plasma prealbumin at 2-5 A resolution. A preliminary report on the polypeptide chain conformation, quaternary structure and thyroxine binding. J Mol Biol 1974; 88: 1-12.

Blake CC, Swan ID, Rerat C, Berthou J, Laurent A, Rerat B. An x-ray study of the subunit structure of prealbumin. J Mol Biol 1971; 61: 217-24.

Blay P, Nilsson C, Owman C, Aldred A, Schreiber G. Transthyretin expression in the rat brain: effect of thyroid functional state and role in thyroxine transport. Brain Res 1993; 632: 114-20.

Bonifacio MJ, Sakaki Y, Saraiva MJ. 'In vitro' amyloid fibril formation from transthyretin: the influence of ions and the amyloidogenicity of TTR variants. Biochim Biophys Acta 1996; 1316: 35-42.

Caroni P. Overexpression of growth-associated proteins in the neurons of adult transgenic mice. Journal of Neuroscience Methods 1997; 71: 3-9.

Coimbra A, Andrade C. Familial amyloid polyneuropathy: an electron microscope study of the peripheral nerve in five cases. I. Interstitial changes. Brain 1971a; 94: 199-206.

Coimbra A, Andrade C. Familial amyloid polyneuropathy: an electron microscope study of the peripheral nerve in five cases. II. Nerve fibre changes. Brain 1971b; 94: 207-12.

Court FA, Brophy PJ, Ribchester RR. Remodeling of motor nerve terminals in demyelinating axons of periaxin-null mice. Glia 2008; 56: 471-9.

Curtis R, Adryan KM, Stark JL, Park JS, Compton DL, Weskamp G, et al. Differential Role of the Low-Affinity Neurotrophin Receptor (P75) in Retrograde Axonal-Transport of the Neurotrophins. Neuron 1995; 14: 1201-1211.

Ducy P, Amling M, Takeda S, Priemel M, Schilling AF, Beil FT, et al. Leptin inhibits bone formation through a hypothalamic relay: a central control of bone mass. Cell 2000; 100: 197-207.

Eipper BA, Stoffers DA, Mains RE. The biosynthesis of neuropeptides: peptide alpha-amidation. Annu Rev Neurosci 1992; 15: 57-85.

Episkopou V, Maeda S, Nishiguchi S, Shimada K, Gaitanaris GA, Gottesman ME, et al. Disruption of the transthyretin gene results in mice with depressed levels of plasma retinol and thyroid hormone. Proc Natl Acad Sci U S A 1993; 90: 2375-9.

Ericsson A, Schalling M, McIntyre KR, Lundberg JM, Larhammar D, Seroogy K, et al. Detection of neuropeptide Y and its mRNA in megakaryocytes: enhanced levels in certain autoimmune mice. Proc Natl Acad Sci U S A 1987; 84: 5585-9.

Fitzgerald M, Nairn P, Bartlett CA, Chung RS, West AK, Beazley LD. Metallothionein-IIA promotes neurite growth via the megalin receptor. Experimental Brain Research 2007; 183: 171-180.

Fleming CE, Mar FM, Franquinho F, Saraiva MJ, Sousa MM. Transthyretin Internalization by Sensory Neurons Is Megalin Mediated and Necessary for Its Neuritogenic Activity. Journal of Neuroscience 2009; 29: 3220-3232.

Fleming CE, Saraiva MJ, Sousa MM. Transthyretin enhances nerve regeneration. J Neurochem 2007; 103: 831-9.

Furtado L, Oliveira F, Furtado E, Geraldes B, Reis A, Viana J, et al. Maximum sharing of cadaver liver grafts composite split and domino liver transplants. Liver Transpl Surg 1999; 5: 157-8.

George R, Griffin JW. Delayed macrophage responses and myelin clearance during Wallerian degeneration in the central nervous system: the dorsal radiculotomy model. Exp Neurol 1994; 129: 225-36.

Gitlin D, Gitlin JD. Fetal and neonatal development of human plasma proteins. In: Putnam FW, editor. The plasma proteins. Vol II. New York: Academic Press, 1975: 264-371.

Grouzmann E, Comoy E, Walker P, Burnier M, Bohuon C, Waeber B, et al. Production and characterization of four anti-neuropeptide Y monoclonal antibodies. Hybridoma 1992; 11: 409-24.

Hansel DE, Eipper BA, Ronnett GV. Neuropeptide Y functions as a neuroproliferative factor. Nature 2001; 410: 940-4.

Hanyu N, Ikeda S, Nakadai A, Yanagisawa N, Powell HC. Peripheral nerve pathological findings in familial amyloid polyneuropathy: a correlative study of proximal sciatic nerve and sural nerve lesions. Ann Neurol 1989; 25: 340-50.

Heilig M. The NPY system in stress, anxiety and depression. Neuropeptides 2004; 38: 213-24.

Hirsch NP. Neuromuscular junction in health and disease. Br J Anaesth 2007; 99: 132-8.

Hosaka H, Nagata A, Yoshida T, Shibata T, Nagao T, Tanaka T, et al. Pancreatic polypeptide is secreted from and controls differentiation through its specific receptors in osteoblastic MC3T3-E1 cells. Peptides 2008; 29: 1390-5.

Howell OW, Doyle K, Goodman JH, Scharfman HE, Herzog H, Pringle A, et al. Neuropeptide Y stimulates neuronal precursor proliferation in the post-natal and adult dentate gyrus. J Neurochem 2005; 93: 560-70.

Johnson EM, Jr., Taniuchi M, Clark HB, Springer JE, Koh S, Tayrien MW, et al. Demonstration of the retrograde transport of nerve growth factor receptor in the peripheral and central nervous system. J Neurosci 1987; 7: 923-9.

Kabat EA, Moore DH, Landow H. An Electrophoretic Study of the Protein Components in Cerebrospinal Fluid and Their Relationship to the Serum Proteins. J Clin Invest 1942; 21: 571-7.

Kanai M, Raz A, Goodman DS. Retinol-binding protein: the transport protein for vitamin A in human plasma. J Clin Invest 1968; 47: 2025-44.

Kanda Y, Goodman DS, Canfield RE, Morgan FJ. The amino acid sequence of human plasma prealbumin. J Biol Chem 1974; 249: 6796-805.

Karga H, Papapetrou PD, Korakovouni A, Papandroulaki F, Polymeris A, Pampouras G. Bone mineral density in hyperthyroidism. Clin Endocrinol (Oxf) 2004; 61: 466-72.

Kato M, Kato K, Blaner WS, Chertow BS, Goodman DS. Plasma and cellular retinoid-binding proteins and transthyretin (prealbumin) are all localized in the islets of Langerhans in the rat. Proc Natl Acad Sci U S A 1985; 82: 2488-92.

Kingery WS, Offley SC, Guo TZ, Davies MF, Clark JD, Jacobs CR. A substance P receptor (NK1) antagonist enhances the widespread osteoporotic effects of sciatic nerve section. Bone 2003; 33: 927-36.

LeBlanc AC, Poduslo JF. Axonal modulation of myelin gene expression in the peripheral nerve. J Neurosci Res 1990; 26: 317-26.

Loun B, Hage DS. Characterization of thyroxine-albumin binding using high-performance affinity chromatography. I. Interactions at the warfarin and indole sites of albumin. J Chromatogr 1992; 579: 225-35.

Madison R, da Silva CF, Dikkes P, Chiu TH, Sidman RL. Increased rate of peripheral nerve regeneration using bioresorbable nerve guides and a laminin-containing gel. Exp Neurol 1985; 88: 767-72.

Mains RE, Cullen EI, May V, Eipper BA. The role of secretory granules in peptide biosynthesis. Ann N Y Acad Sci 1987; 493: 278-91.

Maniatopoulos C, Sodek J, Melcher AH. Bone formation in vitro by stromal cells obtained from bone marrow of young adult rats. Cell Tissue Res 1988; 254: 317-30.

Marques F, Sousa JC, Oliveira P, Oliveira HC, Palha JA. The absence of transthyretin does not impair regulation of lipid and glucose metabolism. Horm Metab Res 2007; 39: 529-33.

Navia JM, Harris SS. Vitamin A influence on calcium metabolism and calcification. Ann N Y Acad Sci 1980; 355: 45-57.

Nunes AF, Liz MA, Franquinho F, Teixeira L, Sousa V, Chenu C, et al. Neuropeptide Y expression and function during osteoblast differentiation - insights from transthyretin knockout mice. FEBS J 2009a.

Nunes AF, Montero M, Franquinho F, Santos SD, Malva J, Zimmer J, et al. Transthyretin knockout mice display decreased susceptibility to AMPA-induced neurodegeneration. Neurochem Int 2009b; 55: 454-7.

Nunes AF, Saraiva MJ, Sousa MM. Transthyretin knockouts are a new mouse model for increased neuropeptide Y. FASEB J 2006; 20: 166-8.

Palha JA. Transthyretin as a thyroid hormone carrier: function revisited. Clin Chem Lab Med 2002; 40: 1292-300.

Palha JA, Episkopou V, Maeda S, Shimada K, Gottesman ME, Saraiva MJ. Thyroid hormone metabolism in a transthyretin-null mouse strain. J Biol Chem 1994; 269: 33135-9.

Palha JA, Fernandes R, de Escobar GM, Episkopou V, Gottesman M, Saraiva MJ. Transthyretin regulates thyroid hormone levels in the choroid plexus, but not in the brain parenchyma: study in a transthyretin-null mouse model. Endocrinology 2000; 141: 3267-72.

Palha JA, Hays MT, Morreale de Escobar G, Episkopou V, Gottesman ME, Saraiva MJ. Transthyretin is not essential for thyroxine to reach the brain and other tissues in transthyretin-null mice. Am J Physiol 1997; 272: E485-93.

Pedrazzini T, Pralong F, Grouzmann E. Neuropeptide Y: the universal soldier. Cell Mol Life Sci 2003; 60: 350-77.

Prigge ST, Mains RE, Eipper BA, Amzel LM. New insights into copper monooxygenases and peptide amidation: structure, mechanism and function. Cell Mol Life Sci 2000; 57: 1236-59.

Quintas A, Saraiva MJ, Brito RM. The tetrameric protein transthyretin dissociates to a non-native monomer in solution. A novel model for amyloidogenesis. J Biol Chem 1999; 274: 32943-9.

Quintas A, Vaz DC, Cardoso I, Saraiva MJ, Brito RM. Tetramer dissociation and monomer partial unfolding precedes protofibril formation in amyloidogenic transthyretin variants. J Biol Chem 2001; 276: 27207-13.

Richardson SJ, Lemkine GF, Alfama G, Hassani Z, Demeneix BA. Cell division and apoptosis in the adult neural stem cell niche are differentially affected in transthyretin null mice. Neurosci Lett 2007; 421: 234-8.

Rogers DC, Fisher EM, Brown SD, Peters J, Hunter AJ, Martin JE. Behavioral and functional analysis of mouse phenotype: SHIRPA, a proposed protocol for comprehensive phenotype assessment. Mamm Genome 1997; 8: 711-3.

Said G, Ropert A, Faux N. Length-dependent degeneration of fibers in Portuguese amyloid polyneuropathy: a clinicopathologic study. Neurology 1984; 34: 1025-32.

Salingcarnboriboon R, Tsuji K, Komori T, Nakashima K, Ezura Y, Noda M. Runx2 is a target of mechanical unloading to alter osteoblastic activity and bone formation in vivo. Endocrinology 2006; 147: 2296-305.

Saraiva MJ, Birken S, Costa PP, Goodman DS. Amyloid fibril protein in familial amyloidotic polyneuropathy, Portuguese type. Definition of molecular abnormality in transthyretin (prealbumin). J Clin Invest 1984; 74: 104-19.

Schafer M, Fruttiger M, Montag D, Schachner M, Martini R. Disruption of the gene for the myelin-associated glycoprotein improves axonal regrowth along myelin in C57BL/Wlds mice. Neuron 1996; 16: 1107-13.

Serot JM, Christmann D, Dubost T, Couturier M. Cerebrospinal fluid transthyretin: aging and late onset Alzheimer's disease. J Neurol Neurosurg Psychiatry 1997; 63: 506-8.

Silva AP, Pinheiro PS, Carvalho AP, Carvalho CM, Jakobsen B, Zimmer J, et al. Activation of neuropeptide Y receptors is neuroprotective against excitotoxicity in organotypic hippocampal slice cultures. Faseb J 2003; 17: 1118-20.

Smith TJ, Davis FB, Deziel MR, Davis PJ, Ramsden DB, Schoenl M. Retinoic acid inhibition of thyroxine binding to human transthyretin. Biochim Biophys Acta 1994; 1199: 76-80.

Sobue G, Nakao N, Murakami K, Yasuda T, Sahashi K, Mitsuma T, et al. Type I familial amyloid polyneuropathy. A pathological study of the peripheral nervous system. Brain 1990; 113 (Pt 4): 903-19.

Soprano DR, Herbert J, Soprano KJ, Schon EA, Goodman DS. Demonstration of transthyretin mRNA in the brain and other extrahepatic tissues in the rat. J Biol Chem 1985; 260: 11793-8.

Sousa JC, Grandela C, Fernandez-Ruiz J, de Miguel R, de Sousa L, Magalhaes AI, et al. Transthyretin is involved in depression-like behaviour and exploratory activity. J Neurochem 2004a; 88: 1052-8.

Sousa MM, Ferrao J, Fernandes R, Guimaraes A, Geraldes JB, Perdigoto R, et al. Deposition and passage of transthyretin through the blood-nerve barrier in recipients of familial amyloid polyneuropathy livers. Lab Invest 2004b; 84: 865-73.

Sousa MM, Monteiro F, Saraiva MJ. Lack of amyloid deposition in the peripheral nervous system of transgenic mice expressing human mutant transthyretin in neurons. FENS Abstracts 2004c; 2: A159.14.

Sousa MM, Norden AG, Jacobsen C, Willnow TE, Christensen EI, Thakker RV, et al. Evidence for the role of megalin in renal uptake of transthyretin. J Biol Chem 2000; 275: 38176-81.

Sousa MM, Saraiva MJ. Neurodegeneration in familial amyloid polyneuropathy: from pathology to molecular signaling. Prog Neurobiol 2003; 71: 385-400.

Takahashi T, Kamiya N, Kawabata N, Takagi M. The effect of retinoic acid on a zinc finger transcription factor, AJ18, during differentiation of a rat clonal preosteoblastic cell line, ROB-C20, into osteoblasts. Arch Oral Biol 2008; 53: 87-94.

Taniuchi M, Clark HB, Schweitzer JB, Johnson EM, Jr. Expression of nerve growth factor receptors by Schwann cells of axotomized peripheral nerves: ultrastructural location, suppression by axonal contact, and binding properties. J Neurosci 1988; 8: 664-81.

van Bennekum AM, Wei S, Gamble MV, Vogel S, Piantedosi R, Gottesman M, et al. Biochemical basis for depressed serum retinol levels in transthyretin-deficient mice. J Biol Chem 2001; 276: 1107-13.

van Jaarsveld PP, Edelhoch H, Goodman DS, Robbins J. The interaction of human plasma retinol-binding protein and prealbumin. J Biol Chem 1973; 248: 4698-705.

Wadhwani KC, Rapoport SI. Transport properties of vertebrate blood-nerve barrier: comparison with blood-brain barrier. Prog Neurobiol 1994; 43: 235-79.

Wang A, Ding X, Sheng S, Yao Z. Retinoic acid inhibits osteogenic differentiation of rat bone marrow stromal cells. Biochem Biophys Res Commun 2008; 375: 435-9.

Wei S, Episkopou V, Piantedosi R, Maeda S, Shimada K, Gottesman ME, et al. Studies on the metabolism of retinol and retinol-binding protein in transthyretin-deficient mice produced by homologous recombination. J Biol Chem 1995; 270: 866-70.

Willnow TE, Hilpert J, Armstrong SA, Rohlmann A, Hammer RE, Burns DK, et al. Defective forebrain development in mice lacking gp330/megalin. Proceedings of the National Academy of Sciences of the United States of America 1996; 93: 8460-8464.

Xapelli S, Silva AP, Ferreira R, Malva JO. Neuropeptide Y can rescue neurons from cell death following the application of an excitotoxic insult with kainate in rat organotypic hippocampal slice cultures. Peptides 2007; 28: 288-94.